Copyright Warning & Restrictions

The copyright law of the United States (Title 17, United States Code) governs the making of photocopies or other reproductions of copyrighted material.

Under certain conditions specified in the law, libraries and archives are authorized to furnish a photocopy or other reproduction. One of these specified conditions is that the photocopy or reproduction is not to be "used for any purpose other than private study, scholarship, or research." If a, user makes a request for, or later uses, a photocopy or reproduction for purposes in excess of "fair use" that user may be liable for copyright infringement,

This institution reserves the right to refuse to accept a copying order if, in its judgment, fulfillment of the order would involve violation of copyright law.

Please Note: The author retains the copyright while the New Jersey Institute of Technology reserves the right to distribute this thesis or dissertation

Printing note: If you do not wish to print this page, then select "Pages from: first page # to: last page #" on the print dialog screen

ABSTRACT

PROCESSING AND CHARACTERIZATION OF GRAPHENE AND GRAPHENE ON SILICON

by
Cheng Peng

Graphene has become a promising material for applications in many areas including electronic devices, batteries and space crafts. Although it has a bright future, the commercial production of graphene has not yet been realized. In this thesis, an overview of the properties and applications of graphene is presented. The early research of preparing graphene and its composites is summarized, which gives the basis to synthesize graphene and improve the process. In this study, graphene oxide (GO) and graphene have been successfully made using graphite; graphene layer has been coated on the surface of a silicon wafer. The resulting specimens are characterized by Raman spectroscopy and Fourier Transform Infrared (FTIR) spectroscopy to identify the composition of the resulting films. Current-Voltage (I-V) measurements are performed to determine the electrical properties of graphene on silicon. Conclusions are made based on the test results.

PROCESSING AND CHARACTERIZATION OF GRAPHENE AND GRAPHENE ON SILICON

by
Cheng Peng

A Thesis
Submitted to the Faculty of
New Jersey Institute of Technology
in Partial Fulfillment of the Requirements for the Degree of
Master of Science in Materials Science and Engineering

Interdisciplinary Program in Materials Science and Engineering

May 2015

APPROVAL PAGE

PROCESSING AND CHARACTERIZATION OF GRAPHENE AND GRAPHENE ON SILICON

Cheng Peng

Dr. Nuggehalli M. Ravindra, Thesis Advisor — Date
Professor, Department of Physics, NJIT
Director, Interdisciplinary Program in Materials Science and Engineering, NJIT

Dr. Michael Jaffe, Committee Member — Date
Research Professor, Department of Biomedical Engineering, NJIT

Mr. Peter Kaufman, Committee Member — Date
President and Chief Technical Officer, PSS Inc.

Dr. Halina Opyrchal, Committee Member — Date
Senior University Lecturer, Department of Physics, NJIT

BIOGRAPHICAL SKETCH

Author: Cheng Peng

Degree: Master of Science

Date: May 2015

Undergraduate and Graduate Education:

- Master of Science in Materials Science and Engineering, New Jersey Institute of Technology, Newark, NJ, 2015

- Bachelor of Science in Materials Science and Engineering, Donghua University, Shanghai, P. R. China, 2013

Major: Materials Science and Engineering

This thesis is dedicated to all my family members.
It is their love and support that has given me the ability to complete this work.

ACKNOWLEDGEMENTS

I express my sincere thanks to all those who have lent me a hand in the course of my writing this thesis. Firstly, I would like to thank my professor and advisor Dr. N.M. Ravindra, who has given me constant advice on my research and has done his best to improve my thesis. I am especially grateful for his mentorship and the knowledge he imparted to me. Secondly, I would like to express my gratitude to my committee members: Dr. Michael Jaffe, Mr. Peter Kaufman and Dr. Halina Opyrchal for their insights and suggestions.

Thanks to my fellow Materials Science and Engineering students at New Jersey Institute of Technology, Yan Liu and Elmostafa Benchafia, who gave me support with the research on coatings and Scanning Electron Microscopy. I thank my friends in the Materials Science & Engineering Program at NJIT; without their help, it would have been harder for me to finish my studies and complete this thesis.

Last but not least, I thank my family for their love and patience. They always had great confidence in me through all these years.

TABLE OF CONTENTS

TABLE OF CONTENTS
(Continued)

TABLE OF CONTENTS
(Continued)

Chapter **Page**

CHAPTER 1

INTRODUCTION

1.1 Background

Due to its excellent properties, graphene offers many unique advantages. It is the thinnest and strongest material ever known in the universe. Its charge carriers exhibit giant intrinsic mobility, have zero effective mass, and can travel for micrometers without scattering at room temperature. Graphene can sustain current densities six orders of magnitude higher than that of copper, shows record thermal conductivity and stiffness, is impermeable to gases, and reconciles such conflicting qualities as brittleness and ductility. Electron transport in graphene is described by a Dirac-like equation, which allows the investigation of relativistic quantum phenomena in a benchtop experiment.

Graphene is a single atomic plane of graphite. It can be sufficiently isolated from its environment to be considered free-standing. Though atomic planes are familiar to us as constituents of bulk crystals, we know so little about one-atom-thick materials such as graphene. This is because nature strictly forbids the growth of low-dimensional crystals [1]. Crystal growth requires high temperatures; therefore, thermal fluctuations are detrimental for the stability of macroscopic one dimensional (1D) and two dimensional (2D) objects. One can grow flat molecules and

nanometer-sized crystallites, but as their lateral size increases, the phonon density integrated over the three dimensional (3D) space available for thermal vibrations rapidly grows, diverging on a macroscopic scale. This forces 2D crystallites to morph into a variety of stable 3D structures.

Though it is challenging to grow 2D crystals in natural environment, it does not actually mean that they cannot be made artificially. Indeed, one can grow a monolayer inside or on top of another crystal and then remove the bulk at sufficiently low temperature, such that the thermal fluctuations are unable to break atomic bonds even in macroscopic 2D crystals and mold them into 3D shapes.

There are two principal routes to make single-layer crystals. The first one is to mechanically split strongly layered materials such as graphite into individual atomic planes. This is the way graphene was made at the beginning. This method is well known as the scotch-tape technique. Regardless of needing significant time and the very detailed process, it does provide high quality crystals, which can reach millimeter size. The other approach is to start with graphitic layers epitaxially grown on top of other crystals [2]. This is the 3D growth during which epitaxial layers remain bound to the underlying substrate and the bond-breaking fluctuations are suppressed. After the epitaxial structure is cooled down, one can remove the substrate by chemical etching. However, it seems too difficult for the single-layer crystal to remain undamaged with this technology. But, recently, this method has been tried by isolating the epitaxial monolayers and transferring onto weakly binding substrates [3-5].

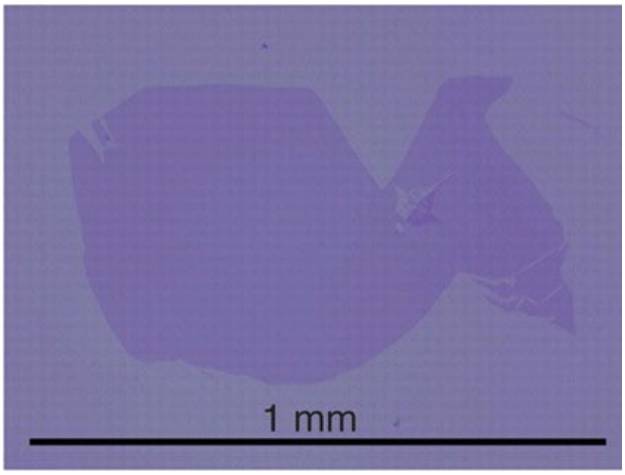

Figure 1.1 Large graphene crystal prepared on an oxidized Si wafer by the scotch-tape technique. [Courtesy of Graphene Industries Ltd.]

Source: K. V. Emtsev et al., Nat. Mater. 8, 203 (2009).

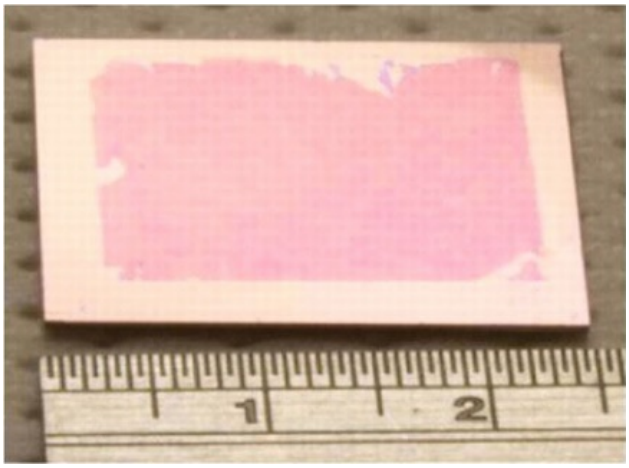

Figure 1.2 The first graphene wafers are now available as polycrystalline one- to five-layer films grown on Ni and transferred onto a Si wafer. [Courtesy of A. Reina and J. Kong, MIT.]

Source: K. V. Emtsev et al., Nat. Mater. 8, 203 (2009).

1.2 Properties

1.2.1 Structure

The graphene honeycomb lattice is composed of two equivalent sub-lattices of carbon atoms bonded together with σ bonds, as shown in Figure 1.3. Each carbon atom in the

lattice has a π orbital that contributes to a delocalized network of electrons. By Monte Carlo simulation and transmission electron microscopy (TEM), we know that freely suspended graphene has 'intrinsic' ripples [6, 7]. Apart from 'intrinsic' corrugations, graphene, in real 3D space, can have other 'defects', including topological defects, vacancies, adatoms, edges/cracks, adsorbed impurities, and so on.

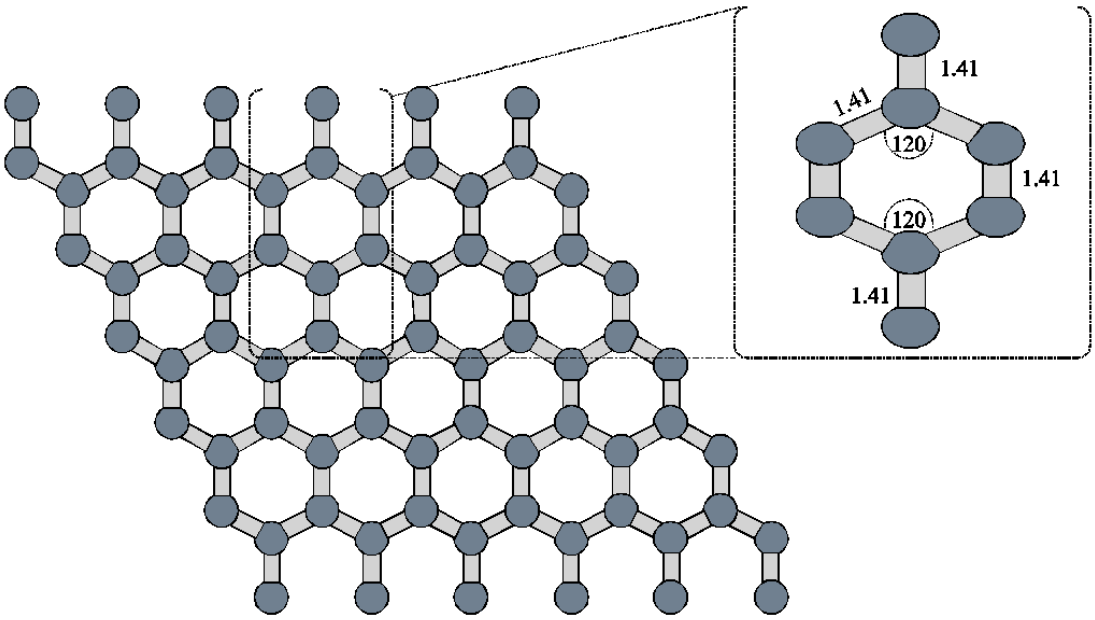

Fig 1.3 Structure of graphene.

Source: Ali Zain Alzahrani (2011). Structural and Electronic Properties of Graphene upon Molecular Adsorption: DFT Comparative Analysis, Graphene Simulation, Prof. Jian Gong (Ed.), ISBN: 978-953-307-556-3, InTech, DOI: 10.5772/20356. Available from: http://www.intechopen.com/books/graphene-simulation/structural-and-electronic-properties-of-graphene-upon-molecular-adsorption-dft-comparative-analysis

1.2.2 Electronic Properties

The most explored aspect of graphene physics is its electronic properties. Unlike common 3D materials, pure graphene is a kind of semimetal or zero gap semiconductor. Scientists have long noticed that, for low energy electrons near the six corners of the 2D

hexagonal Brillouin zone, the energy-momentum is linear dispersion relation [8]:

$$E = \hbar v_F k = \hbar v_F \sqrt{k_x^2 + k_y^2} \tag{1.1}$$

E is energy, ħ is reduced Planck constant, $v_F \approx 106$ is Fermi velocity, k_x and k_y are the x and y axis component of wave vector, respectively.

According to Equation 1.1, the effective mass of electron and electron hole equals zero [9]. Because of this linear dispersion relation, the physical behavior of electrons and holes near these corners can be described by an equation that is formally equivalent to the massless Dirac equation [8, 10]. Therefore, electrons and holes in graphene are called Dirac Fermions; the six corners in Brillouin zone are named Dirac Point, also known as neutral point. This pseudo-relativistic description is restricted to the chiral limit, i.e., to vanishing rest mass M_0, which leads to interesting additional features [1, 11]:

$$v_F \, \vec{\sigma} \cdot \nabla \psi(\mathbf{r}) \; = \; E\psi(\mathbf{r}). \tag{1.2}$$

Here, $v_F \approx 106$ m/s is the Fermi velocity in graphene, $\vec{\sigma}$ is the vector of the Pauli matrices, $\psi(\mathbf{r})$ is the two-component wave function of the electrons, and E is their energy.

1.2.3 Electron Transport

Experimental results from transport measurements show that graphene has a

remarkably high electron mobility at room temperature, with reported values in excess of 15,000$cm^2 \cdot V^{-1} \cdot s^{-1}$ [12]. The symmetry of the conductance data shows that the mobility of electrons and holes should be the same. Moreover, it is nearly independent of temperature between 10K and 100K, which implies that the dominant scattering mechanism is defect scattering. The corresponding resistivity of the graphene sheet would be 10^{-6} $\Omega \cdot cm$. This is less than the resistivity of silver, the lowest known at room temperature. So graphene is an outstanding conductor. Carrier density near the Dirac point is zero; graphene exhibits a minimum conductivity on the order of $4e^2/h$. Also, it may be the perfect material to make any sub-element for a quantum computer.

1.2.4 Optical Properties

According to theory, suspending graphene would absorb white light which is $\pi\alpha \approx 2.3\%$, where α is the fine-structure constant [13]. It is unusual that a single-atom thickness matter has such a high opacity. The unique electron property leads to this property. Even more amazing, the opacity is only related to α, which is normally used only in quantum electrodynamics. The unusual low-energy electronic structure of monolayer graphene features electron and hole conical bands meeting each other at the Dirac point; this is the reason for the high opacity.

Such unique absorption could become saturated when the input optical intensity is above a threshold value. This nonlinear optical behavior is termed saturable absorption and the threshold value is called the saturation fluence. Graphene can be

saturated readily under strong excitation over the visible to near-infrared region, due to the universal optical absorption and zero band gap. This has relevance for the mode locking of fiber lasers, where full band mode locking has been achieved by graphene-based saturable absorber. Due to this special property, graphene has wide applications in ultrafast photonics. Moreover, the optical response of graphene/graphene oxide layers can be tuned electrically [14].

1.2.5 Other Properties

Graphene is an ideal material in spintronics, concerning that its spin-orbit interaction is so little and carbon barely has nuclear magnetic moment. Electrical spin current injection and detection has been demonstrated up to room temperature. Spin coherence length, above one micrometer, at room temperature was observed, and control of the spin current polarity with an electrical gate was observed at low temperature.

Quantum Hall effect only occurs in 2D conductor; this leads to a new metrological standard called resistivity quantum (h/e^2). This e is unit quality of electricity, h is the Planck constant. For a current-carrying conductor, where the current is perpendicular to the applied external magnetic field, its transverse conductivity will become quantized; this is called Hall conductivity. The equation is expressed as:

$$\sigma_{xy} = Ne^2/h \tag{1.3}$$

N is in integers, called Landau level index.

The thermal conductivity of graphene is better than carbon nanotubes (CNTs), which is 5300W/mK. Thermal conductivity of normal CNTs is 3500W/mK. This excellent property makes graphene a promising thermal interface material in large scale nano integrated circuits [29].

In 2014, researchers magnetized graphene by placing it on an atomically smooth layer of magnetic yttrium iron garnet. The electronic properties of graphene were unaffected. Prior approaches involved doping graphene with other substances. The presence of the dopant negatively affected its electronic properties [15].

1.3 Applications

Since the challenges in mass production and large size have been solved step by step, the industrial application of graphene will become more and more real. Based on the research achievements so far, the most likely field would be mobile equipment, aerospace and new energy battery.

Flexible screens are attractive in many recent electronic shows. This is the trend of future development of screens for mobile devices. Flexible screens have broad prospects in future market, with graphene as the basic material. The Korean company, Samsung, has developed glassy flexible screens made with multilayer graphene, as shown in Figure 1.4. It is believed that large scale commercialization can be expected soon.

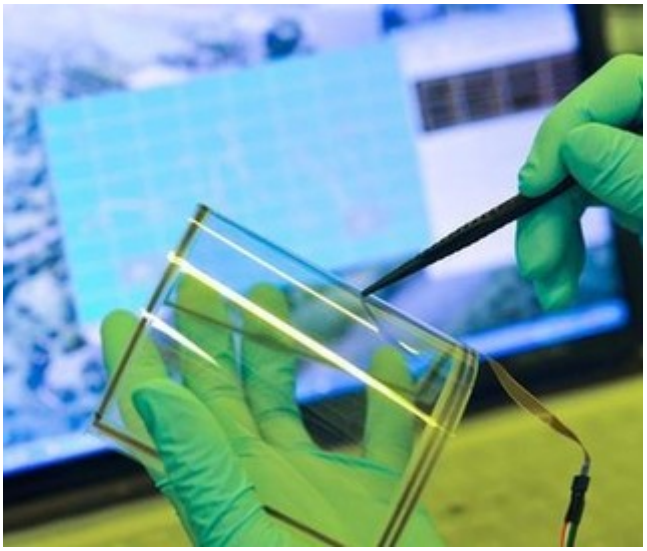

Figure 1.4 Glassy flexible screen made with multilayer graphene.

Source: http://news.hexun.com/2013-01-24/150553242.html

New energy battery is another product based on graphene. Massachusetts Institute of Technology (MIT) has successfully invented flexible photovoltaic panels with graphene layer, which could greatly reduce the cost of flexible solar cells. This kind of solar cell can be used in small electronic devices such as cameras and night vision goggles. Besides, the invention of graphene super cell can also increase the driving distance of electric cars; this has been a serious limitation of electric cars for quite a long time.

Since graphene has the properties of high conductivity, high toughness and is super slim, it has tremendous advantages in applications in aerospace and military related industries. Lately NASA has developed a graphene sensor that can be used on spacecrafts. It can detect microelements in earth's upper atmosphere and find structural defects in aircrafts. Graphene also has potential applications in the field of ultra-light aircraft materials.

CHAPTER 2

EXPERIMENTAL APPROACH

2.1 Research Goal

In this research study, the goal is to synthesize graphene from graphite, make different states of graphene (graphene hydro-gel, aero-gel, film etc.) and pattern graphene on silicon wafers. The idea is to make the patterns to be controllable, including the size and thickness.

2.2 Preparation of Graphene

The first step is to make graphene. The following methods of preparation of graphene have been reported in the literature:

2.2.1 Physical Methods

Scientists who prepare graphene by physical methods usually use low-cost graphite or expandable graphite (EG) as raw material.

Novoselovt et al. used the mechanical cleavage method to obtain graphene from Highly Oriented Pyrolytic Graphite (HOPG) and confirmed the existence of monolayer graphene [16].

Peter W. Sutter et al. used rare metal ruthenium as matrix and “grew” graphene on it, called epitaxy growth method [17].

Liquid and gas phase dissection method is to put graphite or EG in certain organic solvents, using ultrasonic, heating or airflow action to make graphene with certain density [18].

2.2.2 Chemical Methods

Chemical methods are mainly used in laboratories. First, a benzene ring is used as core; after several coupled reactions, bigger aromatic systems are formed and, finally, graphene layer with certain size is formed.

Chemical vapor deposition method involves the introduction of several gases in a reactor at various temperatures and pressures; a new material is formed as the under layer. Utilizing this approach, Srivastava et al. have successfully made graphene on silicon under layer wrapped with nickel [19].

Graphite oxide reduction method is the most potential and promising way to synthesize graphene. It involves the dispersion of graphite sheet into a mixture of various strong acids, such as concentrated nitric acid and concentrated sulfuric acid, followed by the addition of potassium permanganate and the use of ultrasonic to create graphene oxide (GO) hydrosol as shown in Figure 2.1. GO is then reduced to obtain graphene. This is the most common way to prepare graphene. In the present study, this method is used to obtain graphene.

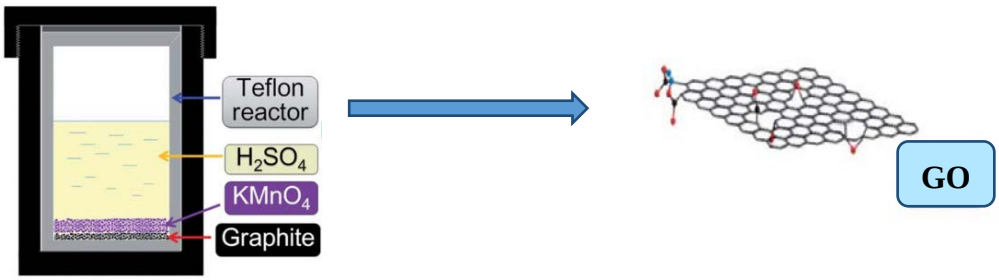

Figure 2.1 Graphite oxide reduction method.

2.2.3 Improved Methods

Normally, there are three methods to make GO: Standenmaier's method, Bordie's method and Hummer's method [20-22]. Daniela C. Marcano et al. used a method basically from Hummer's method and have successfully improved the synthesis process [23]. This improved method, shown in Figure 2.2, provides a greater amount of hydrophilic oxidized graphene material as compared to Hummers' method or Hummers' method with additional $KMnO_4$. This method has been used in the present study.

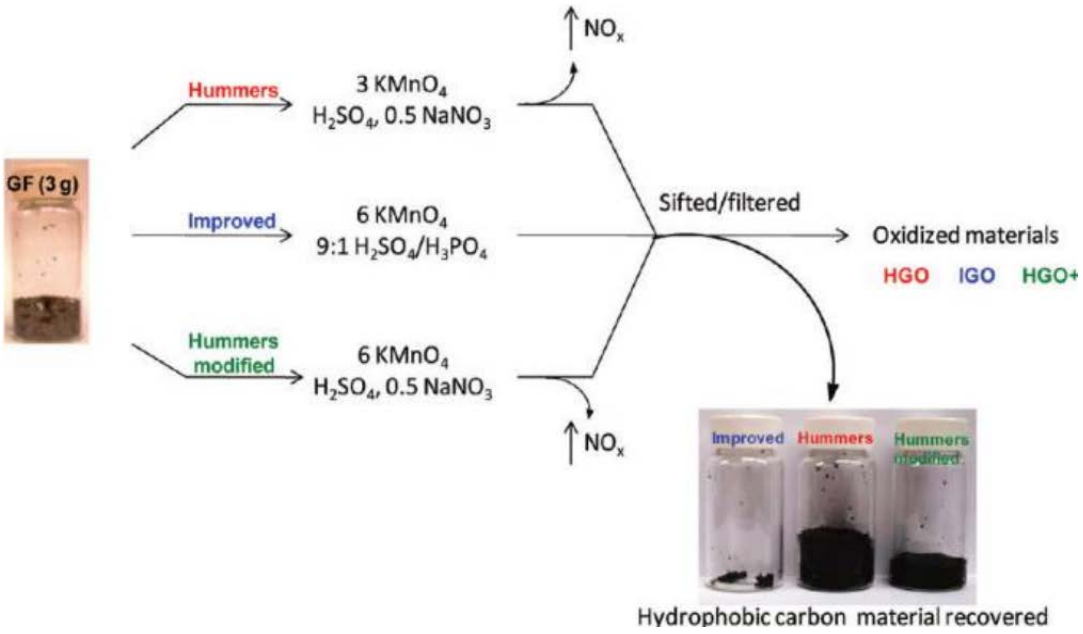

Figure 2.2 Representation of the procedures followed starting with graphite flakes

(GF). Under-oxidized hydrophobic carbon material is recovered during the purification of IGO, HGO, and HGO. The increased efficiency of the IGO method is indicated by the very small amount of under-oxidized material produced.

Source: Marcano, D. C., Kosynkin, D. V., Berlin, J. M., Slesarev, A., Alemany, L. B., Lu, W., Tour, J. M., Improved Synthesis of Graphene Oxide, AcsNano, 4, 8, 4806-4814, (2010).

2.3 Preparation of Graphene Sol-Gel

Hydrogels and aerogels are two typical kinds of 3D macroscopic assemblies. They consist of microporous and mesoporous networks that allow access and diffusion of ions and molecules, offer attractive potentials for applications in electrode materials, catalysis and water treatment.

2.3.1 Hydrogel

Self-assembly has been recognized as one of the most powerful techniques for integrating various nanostructured building blocks into macroscopic materials that can translate properties at the nanoscale into resulting macroscopic devices with hierarchical microstructures and novel functionalities. Furthermore, the assembled superstructures are of novel collective physiochemical properties that are different from individual components and the bulk material, which enriches the species in the materials field and improves their capacities for practical applications [24, 25].

SHENG Kai-xuan et al. fabricated graphene hydro-gel via chemical reduction of graphene oxide with sodium ascorbate [26]. A photograph of an aqueous mixture of GO with sodium ascorbate and the SEM image are shown in Figure 2.3.

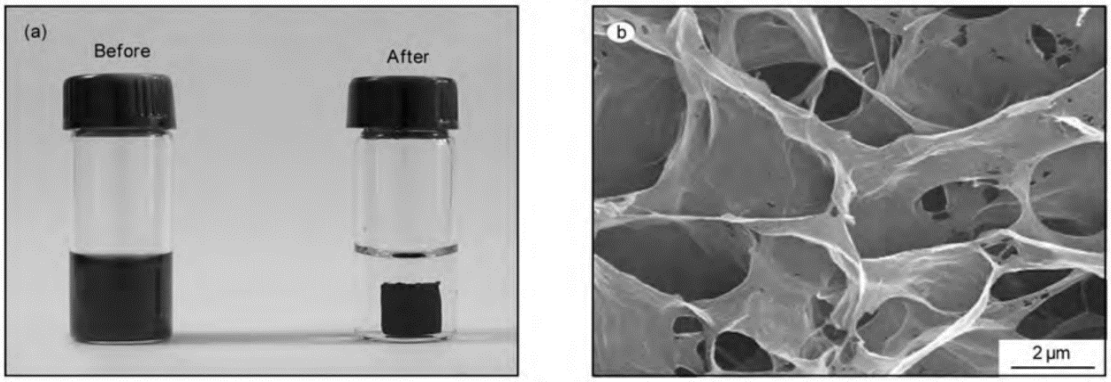

Figure 2.3 (a) Photograph of an aqueous mixture of GO (2 mg· mL-1) and sodium ascorbate before (left) and after (right) chemical reduction at 90^{o}C for 1.5 h. (b) SEM image of SGHs.

Source: Sheng, K. X., Xu, Y. X., Li, C., Shi, G. Q., High-performance self-assembled graphene hydrogels prepared by chemical reduction of graphene oxide, New Carbon Materials, 2, 9-15, (2011).

2.3.2 Aerogel

In March, 2013, Professor Gao C et al. [27], from Zhejiang University, China, made a material which is super light (shown in Figure 2.4). They called it carbon sponge. In fact, it is a graphene aerogel, one of the lightest materials in the world. It only weighs 0.16mg/cm^3, even lighter than helium.

Graphene can change its shape optionally and has very good elastic properties, which can be compressed 80% and return to its original shape. Graphene aerogel has a very high and quick adsorption capacity for organic solvents. It can adsorb oil that weighs 900 times heavier than itself without adsorbing water. With this property, carbon sponge can be used to deal with oil spill in the sea. Moreover, graphene aerogel is the ideal material for energy storage, insulation, catalyst carrier and high-performance composites.

Figure 2.4 Graphene aerogel.

Source:http://baike.baidu.com/picture/10346843/10515620/0/0dd7912397dda1449ca563c3b3b7d0a20cf48616.html?fr=lemma&ct=single#aid=0&pic=0dd7912397dda1449ca563c3b3b7d0a20cf48616

In order to make graphene aerogel, it would be much easier if it begins with the hydrogel. The only step is to lyophilize the graphene hydrogel. In this study, graphene hydrogel was processed; this was followed by the formation of aerogel.

2.4 Preparation of Coatings on Silicon

Tetra-valent silicon is relatively inert, but still reacts with halogens and dilute alkalis, but most acids (except for some hyper-reactive combinations of nitric acid and hydrofluoric acid) have no known effect on it. So the reduction of GO directly on the surface of a silicon wafer requires a non-alkaline condition. It means that the normal way of using hydrazine hydrate ($N_2H_4 \cdot H_2O$) is not practicable here, because it needs an

alkaline environment. Also, high temperature reduction (HTR) is not fit for lab preparation, as it needs more than 1000^{o}C and can be quite dangerous.

Therefore, a new method was found to reduce GO in a weak acid environment, which can be done in a lower temperature (under 100^{o}C). According to the Metal Institute of the Chinese Academy of Sciences, hydroiodic acid (HI) can be used to reduce GO effectively in a one-step reaction [28].

CHAPTER 3

RAW MATERIALS AND CHARACTERIZATION METHODS

3.1 Preparation of GO

The following raw materials are used in this study: Natural graphite powder (1000 mesh, 15μm), potassium permanganate ($KMnO_4$), hydrochloric acid (HCl), sulfuric acid (H_2SO_4, 98%), sodium nitrate ($NaNO_3$), hydrogen peroxide (H_2O_2, 30%) deionized water and anhydrous ethanol.

The following equipment and lab supplies are used: Beakers of different sizes, measuring cylinders of different sizes, several droppers, three-necked flask, iron support, funnel and separator funnel, water bath cauldron, ultrasonic instrument, vacuum oven, centrifuge, electronic scale, agitator.

3.2 Preparation of Graphene Sol-Gel

The following raw materials are used: Graphene oxide (made earlier), deionized water, sodium ascorbate, ammonia solution.

The following equipment and lab supplies are used: Beakers of different sizes, droppers, ultrasonic instrument, vacuum oven, freezing dryer.

3.3 For Graphene Coating on Silicon

The following raw materials are used: Graphene oxide (made earlier), deionized water, hydroiodic acid (HI, 57%wt), saturated sodium bicarbonate (5×100 ml), acetone (2×100 ml), acetic acid.

The following equipment and lab supplies are used: Beakers, droppers, ultrasonic instrument, vacuum oven.

3.4 Methods of Characterization

3.4.1 Raman Spectra

Raman spectroscopy is a spectroscopic technique used to observe vibrational, rotational, and other low-frequency modes in a system [30]. Raman spectroscopy is commonly used in chemistry to provide a fingerprint by which molecules can be identified.

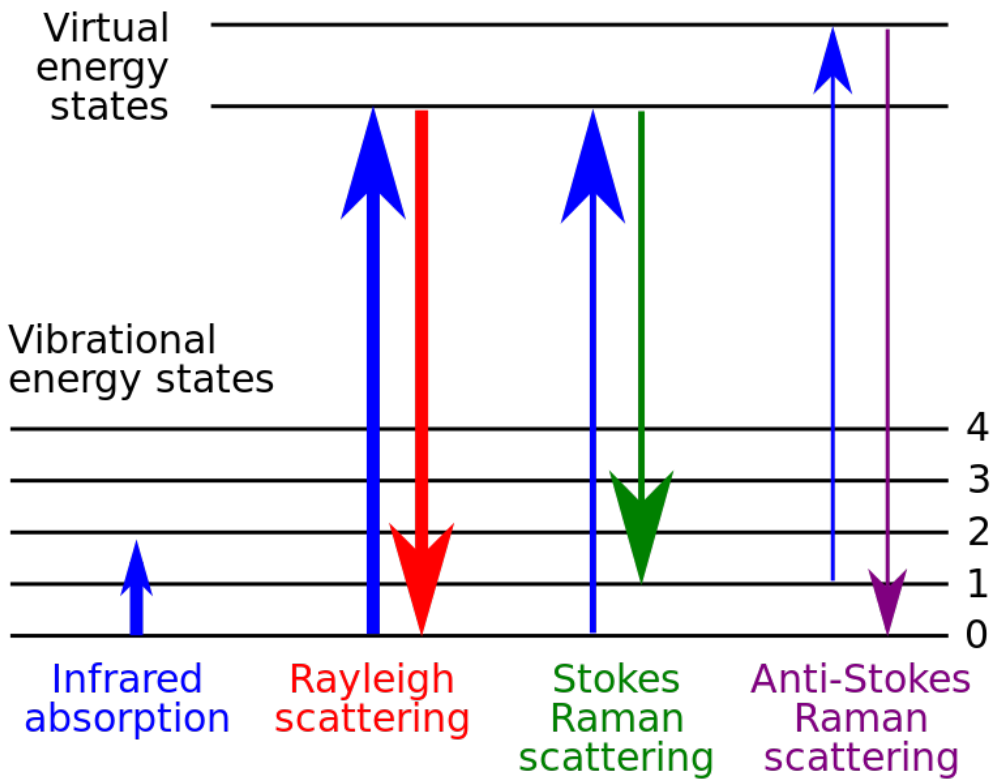

Figure 3.1 Raman spectra

Source:http://upload.wikimedia.org/wikipedia/commons/thumb/4/41/Raman_energy_levels.svg/850px-Raman_energy_levels.svg.png

Raman Spectroscopy relies on inelastic scattering or Raman scattering, of monochromatic light, usually from a laser in the visible, near infrared, or near ultraviolet range. The laser light interacts with molecular vibrations, phonons or other excitations in the system, resulting in the energy of the laser photons being shifted up or down. The shift in energy gives information about the vibrational modes in the system. Infrared spectroscopy yields similar, but complementary information.

Typically, a sample is illuminated with a laser beam. Electromagnetic radiation from the illuminated spot is collected with a lens and sent through a monochromator. Elastic scattered radiation at the wavelength corresponding to the laser line (Rayleigh

scattering) is filtered out, while the rest of the collected light is dispersed onto a detector by either a notch filter or a band pass filter.

The Raman Effect occurs when electromagnetic radiation impinges on a molecule and interacts with the polarizable electron density and the bonds of the molecule in the phase (solid, liquid or gaseous) and environment in which the molecule finds itself. For spontaneous Raman effect, which is a form of inelastic light scattering, a photon (electromagnetic radiation of a specific wavelength) excites (interacts with) the molecule in either the ground rovibronic state (lowest rotational and vibrational energy level of the ground electronic state) or an excited rovibronic state. This results in the molecule being in a so-called virtual energy state for a short period of time before an inelastically scattered photon results. The resulting inelastically scattered photon which is "emitted"/"scattered" can be of either lower (Stokes) or higher (anti-Stokes) energy than the incoming photon. In Raman scattering, the resulting rovibronic state of the molecule is a different rotational or vibrational state than the one in which the molecule was originally, before interacting with the incoming photon (electromagnetic radiation). The difference in energy between the original rovibronic state and this resulting rovibronic state leads to a shift in the emitted photon frequency away from the excitation wavelength, the so-called Rayleigh line. The Raman Effect is due to inelastic scattering and should not be confused with emission (fluorescence or phosphorescence) where a molecule in an excited electronic state

emits a photon of energy and returns to the ground electronic state, in many cases to a vibrationally excited state on the ground electronic state potential energy surface.

If the final vibrational state of the molecule is more energetic than the initial state, the inelastically scattered photon will be shifted to a lower frequency for the total energy of the system to remain balanced. This shift in frequency is designated as a Stokes shift. If the final vibrational state is less energetic than the initial state, then the inelastically scattered photon will be shifted to a higher frequency, and this is designated as an anti-Stokes shift. Raman scattering is an example of inelastic scattering because of the energy and momentum transfer between the photons and the molecules during the interaction. Rayleigh scattering is an example of elastic scattering, the energy of the scattered Rayleigh scattering is of the same frequency (wavelength) as the incoming electromagnetic radiation.

A change in the molecular electric dipole-electric polarizability with respect to the vibrational coordinate corresponding to the rovibronic state is required for a molecule to exhibit Raman Effect. The intensity of the Raman scattering is proportional to the electric dipole-electric dipole polarizability change. The Raman spectra (Raman scattering intensity as a function of the Stokes and anti-Stokes frequency shifts) is dependent on the rovibronic (rotational and vibrational energy levels of the ground electronic state) states of the sample. This dependence on the electric dipole-electric dipole polarizability derivative differs from infrared spectroscopy where the interaction between the molecule and light is determined by

the electric dipole moment derivative, the so-called atomic polar tensor (APT); this contrasting feature allows one to analyze transitions that might not be IR active via Raman spectroscopy, as exemplified by the rule of mutual exclusion in centrosymmetric molecules. Bands which have large Raman intensities in many cases have weak infrared intensities and vice versa. For very symmetric molecules, certain vibrations may be both infrared and Raman inactive (within the harmonic approximation). In those instances, one can use the technique of inelastic incoherent neutron scattering to determine the vibrational frequencies. The selection rules for inelastic incoherent neutron scattering (IINS) are different from those of both infrared and Raman scattering. Hence, the three types of vibrational spectroscopy are complementary, all giving in theory the same frequency for a given vibrational transition, but the relative intensities giving different information due to the types of interaction between the molecule and the electromagnetic radiation for infrared and Raman spectroscopy and with the neutron beam for IINS.

3.4.2 Fourier Transform Infrared (FTIR) Spectroscopy

Fourier transform infrared spectroscopy (FTIR) is a technique which is used to obtain an infrared spectrum of absorption, emission, photoconductivity or Raman scattering of a solid, liquid or gas [31]. An FTIR spectrometer simultaneously collects high spectral resolution data over a wide spectral range. This confers a significant advantage over a dispersive spectrometer which measures intensity over a narrow range of wavelengths at a time.

The goal of FTIR is to measure how well a sample absorbs light at each wavelength. The most straightforward way to do this, the "dispersive spectroscopy" technique, is to shine a monochromatic light beam at a sample, measure how much of the light is absorbed, and repeat for each different wavelength.

Fourier transform infrared spectroscopy is a less intuitive way to obtain the same information. Rather than shining a monochromatic beam of light at the sample, this technique shines a beam containing many frequencies of light at once, and measures how much of that beam is absorbed by the sample. Next, the beam is modified to contain a different combination of frequencies, giving a second data point. This process is repeated many times. Afterwards, a computer takes all these data and works backwards to infer what the absorption is at each wavelength.

The beam described above is generated by starting with a broadband light source—one containing the full spectrum of wavelengths to be measured. The light shines into a Michelson interferometer—a certain configuration of mirrors, one of

which is moved by a motor. As this mirror moves, each wavelength of light in the beam is periodically blocked, transmitted, blocked, transmitted, by the interferometer, due to wave interference. Different wavelengths are modulated at different rates, so that at each moment, the beam coming out of the interferometer has a different spectrum.

As mentioned earlier, computer processing is required to turn the raw data (light absorption for each mirror position) into the desired result (light absorption for each wavelength). The processing required turns out to be a common algorithm called the Fourier transform. The raw data is sometimes called an "interferogram".

3.5 Apparatus

The following equipment was used for the characterization: Thermo DXR Raman spectra microscopy (from USA); Vector 22 FTIR spectroscope (Bruker from Switzerland) - shown in Figure 3.2.

Figure 3.2 Thermo DXR and Vector 22.

CHAPTER 4

EXPERIMENTS AND CHARACTERIZATION

4.1 Preparation of GO

Gaphene oxide was prepared basically using hummer's method; meanwhile, we also changed some parameters to increase the productivity and success ratio.

Concentrated H_2SO_4 (69 mL) was added to a mixture of graphite flakes (3.0 g, 1 wt equiv) and NaNO3 (1.5 g, 0.5 wt equiv), and the mixture was cooled to 0 °C using ice water bath.

$KMnO_4$ (15-18 g, 5-6 wt equiv) was added slowly with a funnel in portions to keep the reaction temperature below 20 °C.

The reaction beaker was warmed to 35 °C and stirred for 6 hours, at which time water (138 mL) was added slowly with a separator funnel, producing a large exotherm to 98 °C, as shown in Figure 4.1.

Figure 4.1 Processing of GO.

External heating was introduced by hot water bath to maintain the reaction temperature at 98 °C for 15 minutes; then the heat was removed and the reaction beaker was cooled using a water bath until the temperature dropped down below 10^{o}C.

Additional water (420 mL) and 30% H_2O_2 (3 mL) were added, producing another exotherm. With the added H_2O_2, the suspension liquid turned golden yellow, as shown in Figure 4.2.

Figure 4.2 Suspension liquid before (right) and after (left) H_2O_2 was added.

After air cooling, hydrochloric acid (HCl) was added to the mixture to remove the rest of H_2O_2. Centrifuge was used to wash GO with anhydrous ethanol as solvent for three to five times, until the PH approached 7. Upper clear liquid was removed leaving behind the mud-like graphene oxide.

GO was taken out and spread on a tinfoil in a tray. The tray was put into the vacuum oven at the temperature of 40^{o}C for 24 hours. Then the GO dispersion was prepared as shown in Figure 4.3.

Figure 4.3 Graphene oxide.

4.2 Preparation of Graphene Sol-Gel.

The second part is to make the graphene oxide (GO) into hydrogel. GO powders were added to deionized water. Using ultra-sound and strong mechanical stirring for 2 hours, GO was made into an aqueous dispersion (2mg/ml). 10ml of GO aqueous dispersion was put in a glass vial. Then, 40mg sodium ascorbate was added. After sonication for 5 minutes to dissolve the sodium ascorbate, a homogeneous yellow-brown dispersion

was obtained. This dispersion was heated in a drying oven at 90^{o}C for 1.5 hours to produce the self-assembled graphene hydrogels (SGH), as shown in Figure 4.4.

Figure 4.4 Graphene hydrogel.

The graphene hydrogel was put in a chamber containing ammonia, at room temperature, for 24 hours. It was lyophilized in a freezing dryer. Then graphene aerogel was prepared as shown in Figure 4.5.

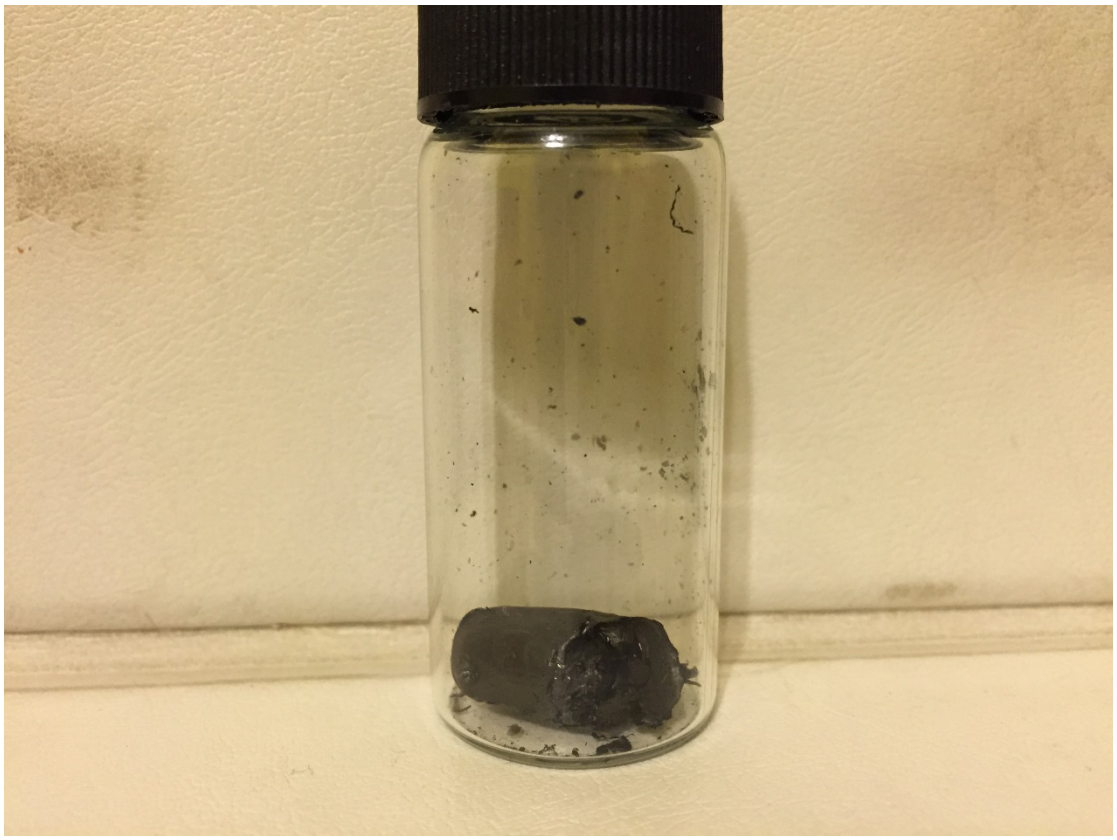

Figure 4.5 Graphene aerogel.

4.3 Coating on Silicon Wafer

4.0g of GO was dispersed in 1.5L of acetic acid. This dispersion was subjected to ultrasonic frequencies in an ultrasonic bath cleaner until it became clear. HI (80.0 ml) was then added and the mixture was stored at 40 °C for 40 hours with constant stirring. Then the product was isolated by filtration, washed with saturated sodium bicarbonate (5×100 ml), distilled water (5×100 ml) and acetone (2×100 ml). A homogeneous liquid

dispersion was formed in the ultrasonic bath. Small droplets of the liquid were dropped on the surface of the silicon wafer. The wafers were vacuum dried overnight, at room temperature, to yield reduced graphene oxide on silicon wafers.

4.4 Characterization

The prepared GO samples were characterized by Raman spectroscopy and FTIR to identify the ingredients. The microstructures of graphene sol-gel were obtained by Scanning Electron Microscopy. Current-Voltage (I-V) measurements were made to analyze the electrical properties of graphene on silicon.

CHAPTER 5

DATA ANALYSIS AND CHARACTERIZATION

5.1 Analysis of Raman Spectra

In graphene, the Stokes phonon energy shift, caused by laser excitation, creates two main peaks in the Raman spectrum: G (1580cm^{-1}), a primary in-plane vibrational mode, and 2D (2690cm^{-1}), a second-order overtone of a different in plane vibration, D (1350cm^{-1}) [32]. D and 2D peak positions are dispersive depending on the laser excitation energy.

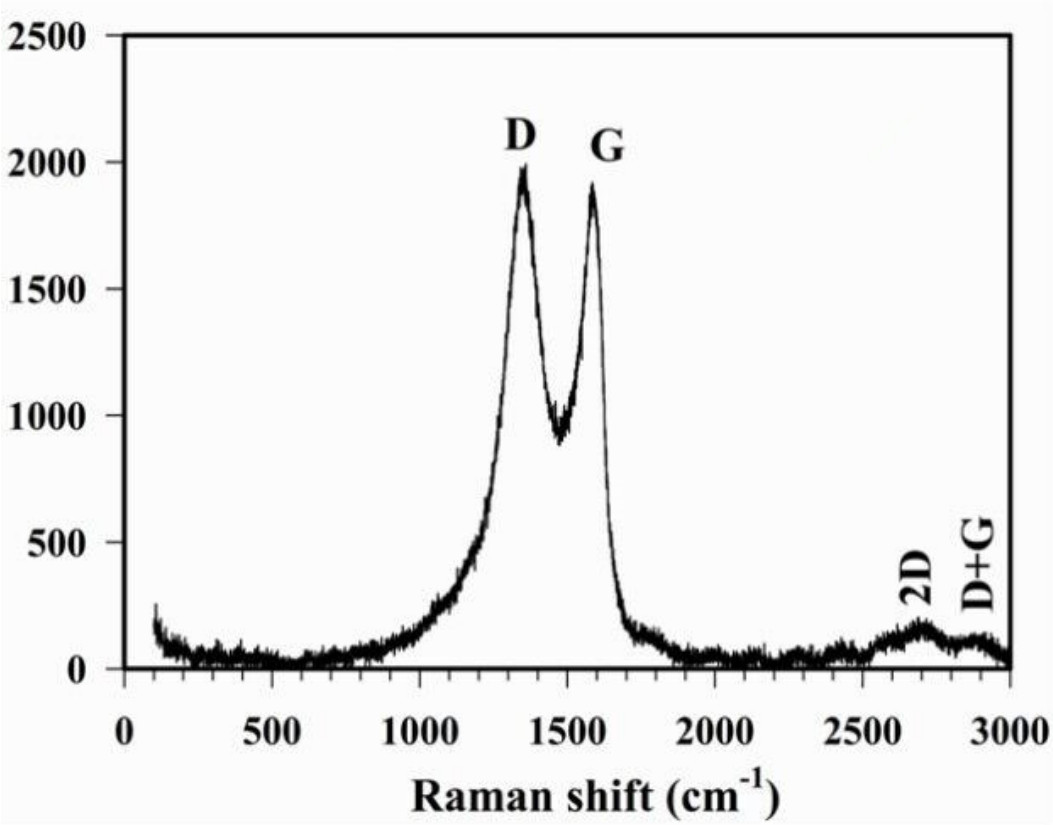

Figure 5.1 Typical Raman spectrum of graphene oxide [33].

Source: Shahriary, L., Athawale, A. A., Graphene Oxide Synthesized by using Modified Hummers Approach, International Journal of Renewable Energy and Environmental Engineering, ISSN 2348-0157, 02, 01, (2014).

In Graphene Oxide, the main features in the Raman spectra are the G and D peaks and their overtones. As shown in Figure 5.1, the first-order G and D peaks, both arising from the vibrations of sp2 carbon, appear at around 1580 cm^{-1} and 1350 cm^{-1}, respectively. The G peak correspond to the optical E_{2g} phonons at the Brillouin zone center resulting from the bond stretching of sp^2 carbon pairs in both, rings and chains. G peak would also increase with the larger number of layers. The D peak represents the breathing mode of aromatic rings arising due to defect in the sample. Therefore, the D peak intensity is often used as a measure of the degree of disorder [33]. The 2D peak is attributed to double resonance transitions resulting in the production of two phonons with opposite momentum. Besides, unlike the D peak, which is Raman active only in presence of defects, the 2D peak is active even in the absence of any defects.

Raman spectrum of GO is shown in Figure 5.2 after the baseline was corrected.

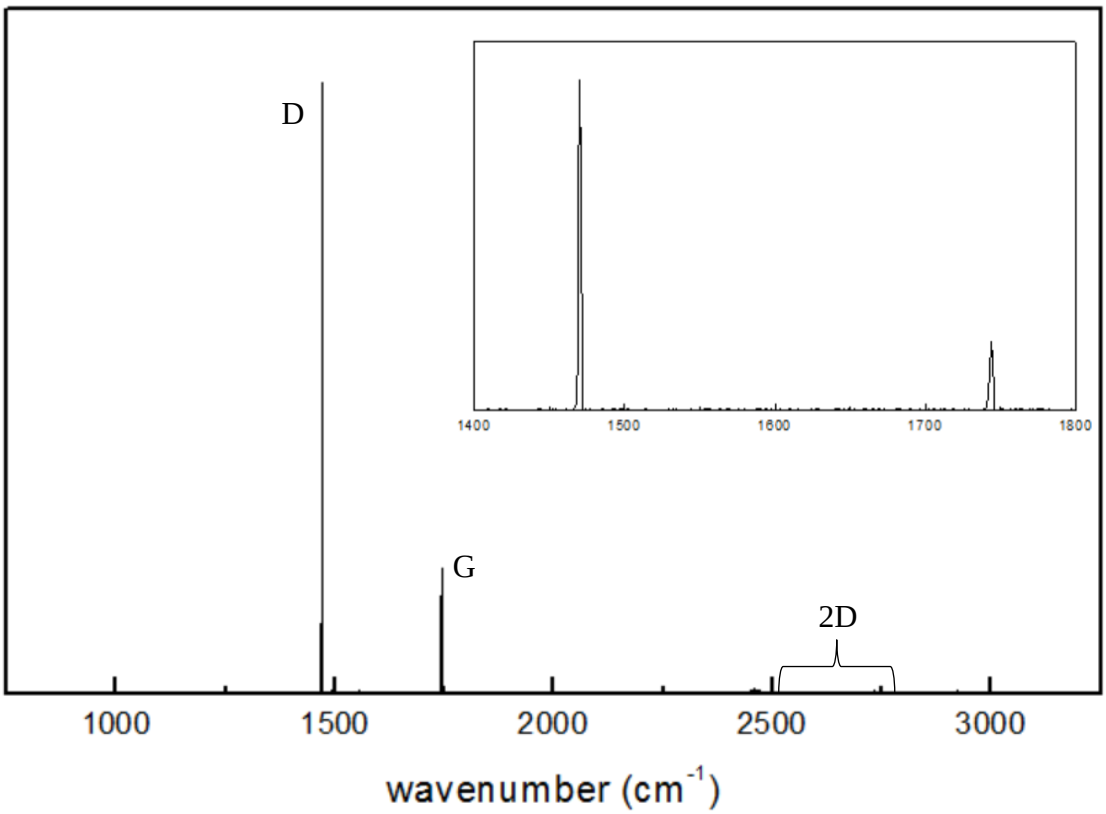

Figure 5.2 Raman spectrum of GO.

The first-order D peak itself is not visible in pristine graphene because of crystal symmetries. In GO, the charge carriers are excited and inelastically-scattered by a phonon. In Figure 5.2, the prominent D peak at ~1480cm^{-1} and the G peak at ~1750cm^{-1} are indicative of significant structural disorder in GO. Weak and broad 2D peaks are another indication of disorder. As the GO samples that were made had very small crystal size, the amount of disorder can be very high, which leads to very strong D peaks.

Figure 5.2 shows that graphene oxide of high degree of dispersion has been prepared successfully. Combined with the results of the FTIR spectra, a more accurate characterization will be made.

5.2 Analysis of FTIR

Figure 5.3 shows sample FTIR spectra from the literature [34]. While no significant peak was found in graphite, the presence of different types of oxygen functionalities in graphene oxide was confirmed at 3430 cm^{-1} (-OH stretching vibrations), at 1725 cm^{-1} (stretching vibrations from C=O), at 1618 cm^{-1} (skeletal vibrations from unoxidized graphitic domains), at 1225 cm^{-1} (C-OH stretching vibrations), and at 1057 cm^{-1} (C-O stretching vibrations). The peak in the FTIR spectra of reduced graphene shows that the -OH stretching vibrations, observed at 3430 cm^{-1}, was significantly reduced due to deoxygenation. While stretching vibrations from C=O at 1720 cm^{-1} were still observed, they were caused by the remaining carboxyl groups.

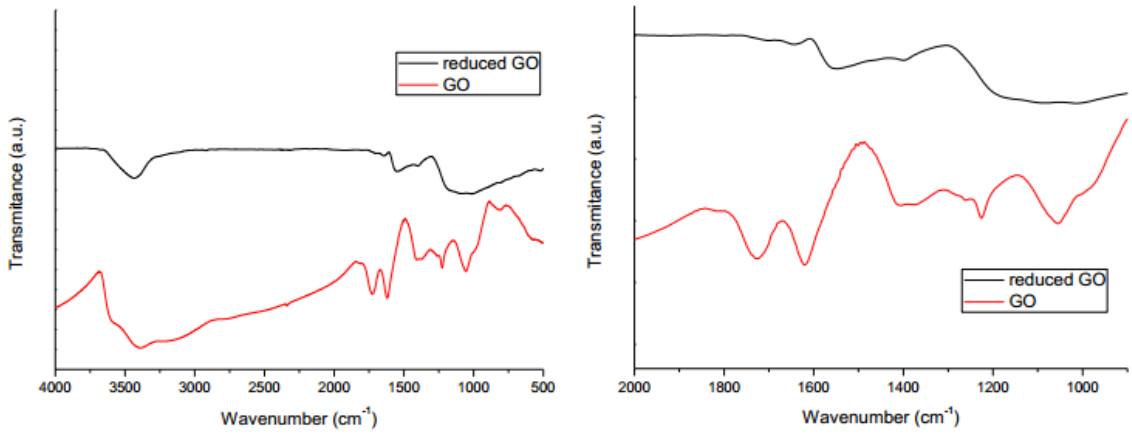

Figure 5.3 Assignation (cm^{-1}): for graphene oxide 1725 C=O (carbonyl/carboxy); 1618 C=C (aromatics); 1407 C-O (carboxy); 1225 C-O (epoxy); 1057 C-O (alkoxy). The peaks of the oxygen functional groups become weaker, showing that they are almost entirely removed in reduced graphene oxide.

Source: Nanoinnova Technologies SL http://www.nanoinnova.com/Uploads/Features/7665255.pdf (accessed March 10, 2015).

After data collection of FTIR, the GO and rGO curves were put together to make it more intuitive to analyze, as shown in Figure 5.4.

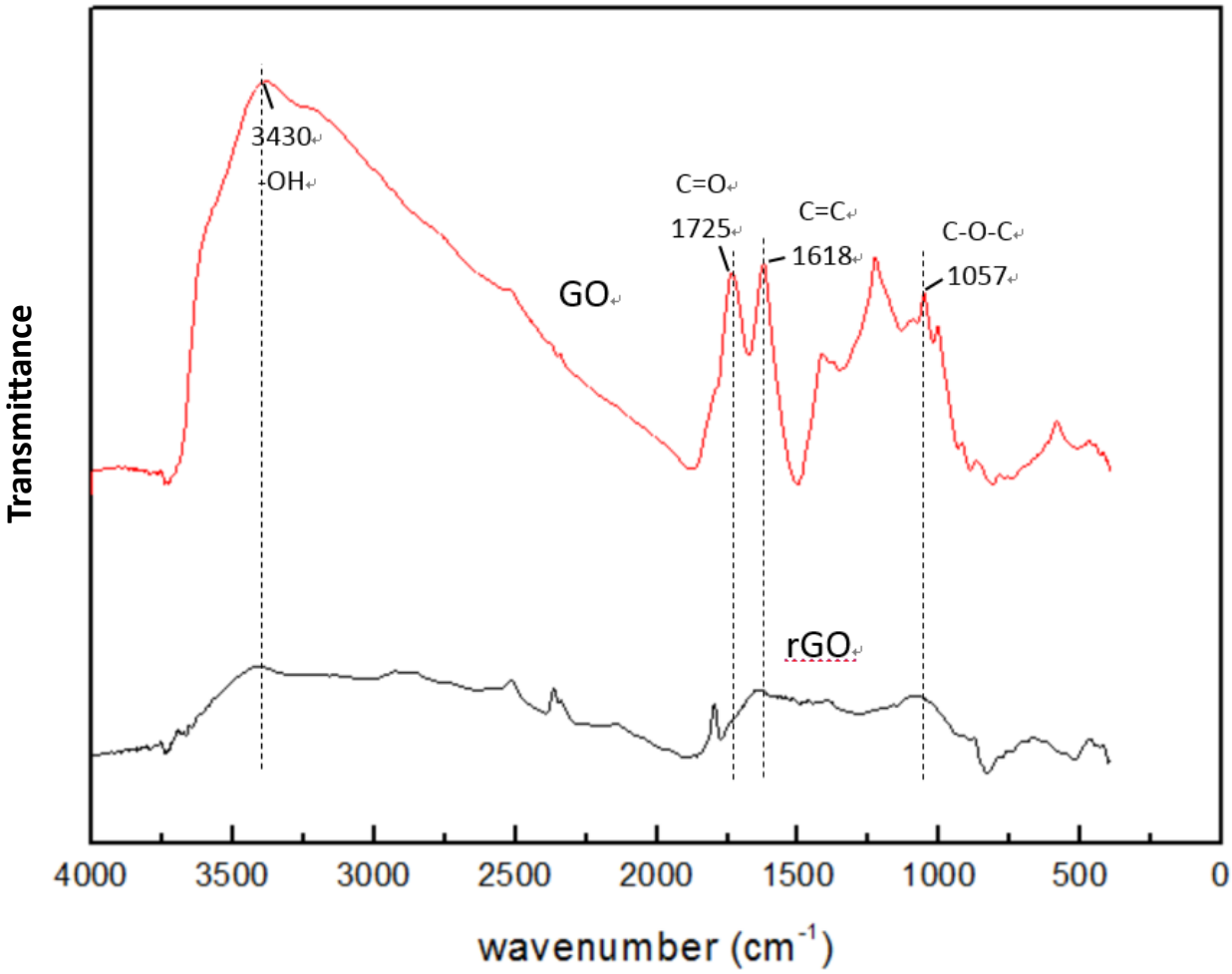

Figure 5.4 FTIR spectra of GO and reduced GO.

As can be seen in Figure 5.4, for GO, there is a wide, strong absorption peak near 3430cm^{-1}, which is the stretching vibration peak of hydroxyl groups (-OH). The peak near 1725cm^{-1} is due to C=O in the carboxyl group of GO. The peak next to it is the absorption peak of C=C groups near 1618cm^{-1}. The peak near 1057cm^{-1} is due to the vibration peak of C-O-C groups. The spectra of GO indicates that there are at least –OH, -C=C, C-O-C and –C=O groups existing in the graphene oxide that was processed in this study. These results are in accord with the structure of GO reported in the literature.

The presence of these oxygen-containing groups reveals that the graphene has been successfully oxidized. The polar groups, especially the surface hydroxyl groups, result in the formation of hydrogen bonds between graphite and water molecules; this further explains the hydrophilic nature of graphene oxide.

When graphene oxide is restored into rGO, the peak near 3430cm^{-1} decreases sharply, and so does the C=O peak near 1725cm^{-1}. This phenomenon shows that the graphene oxide was well restored by the process that was considered in this study. Meanwhile, it can be found that the peaks near 1618cm^{-1} and 1057cm^{-1} of C=C and C-O-C also became weaker, which further verified the decrease in the content of oxygen, suggesting the success of preparing graphene sol-gel. However, it is impossible to get rid of all the oxygen during the reduction of GO; so the graphene that was made in this study still had some oxygen-containing groups in it.

5.3 Scanning Electron Microscopy (SEM) Studies of Graphene Sol-Gel

The microstructures of graphene sol-gel were studied by scanning electron microscopy (SEM). The micrographs are shown in Figure 5.5.

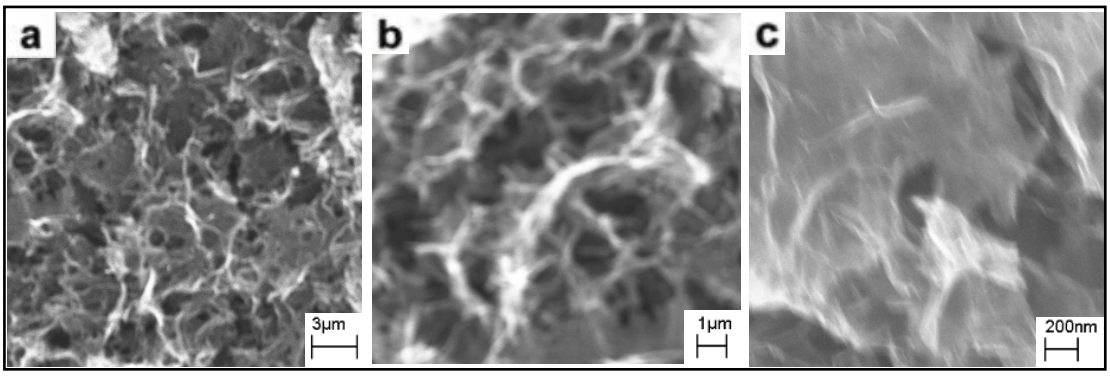

Figure 5.5 (a-c) SEM images with different magnifications of the Graphene sol-gel interior microstructures.

The sol-gel has a well-defined and interconnected 3D porous network as can be seen in SEM micrographs. The pore sizes are from less than 1micrometer to several micrometers. The walls of the pores are composed of stacked graphene sheets, which contribute to the cross-linked structure of graphene sol-gel. This structure is also the main reason why the sol-gel is light in weight and flexible.

5.4 Electrical Properties of Graphene on Silicon

In the past few years, developing carbon nanotube (CNT)-silicon solar cells has been a growing interest. After several efforts by scientists, the power conversion efficiency has continuously improved to the range of 10-15%. The devices are typically made by depositing a transparent single-walled CNT film on the surface of a single-crystal Si wafer to form CNT-Si junction and subsequent chemical doping on the CNT film and

junction to optimize electronic property. Compared to traditional Si solar cells involving high-temperature dopant diffusion and additional metal grids as top contacts, the fabrication of CNT-Si heterojunctions is a low-temperature process based on commercial wafers while still leading to high efficiency [35].

Figure 5.6 Electrical characterization of Graphene-Si.

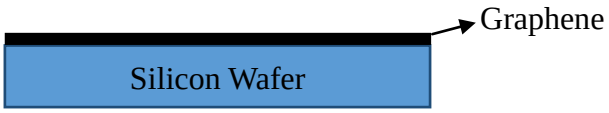

When it comes to graphene, it can be considered as a structure obtained by unrolling a CNT into a flat sheet. As shown in Figure 5.6, it is also practicable to make Graphene-Silicon solar cells. In fact, the 2D structure, atomic thickness, and high carrier mobility make graphene an ideal electrode material to be applied in a variety of thin film devices. Since CNT-Si solar cell has been a success, it is anticipated that the Graphene-Si solar cell should also perform well.

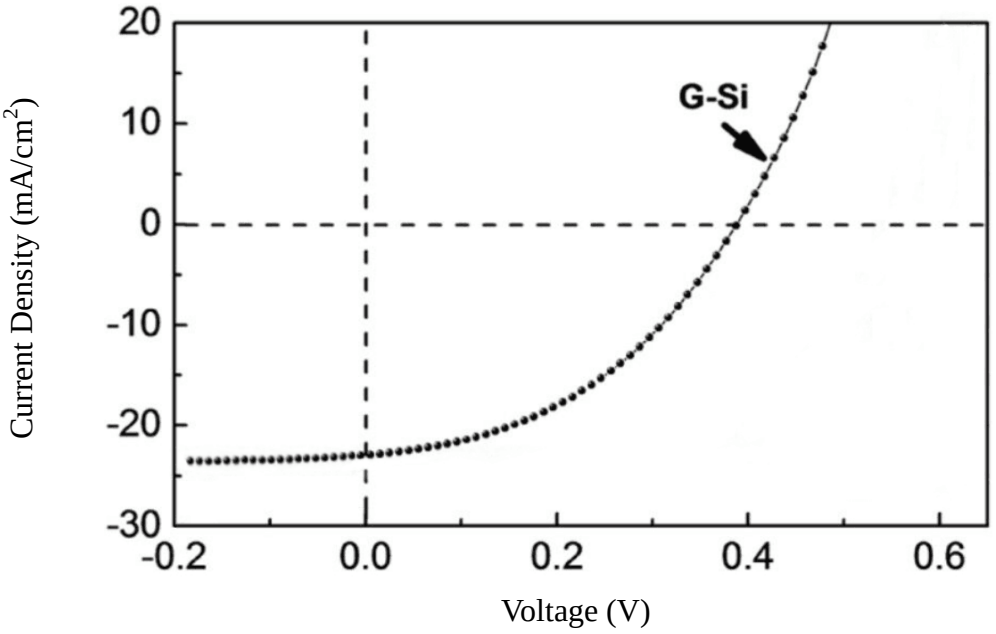

Figure 5.7 J−V characteristics of Graphene on Silicon. Current Density (mA/cm^2)

Figure 5.7 shows the J-V characteristics of graphene/silicon (G-Si). As can be seen in the figure, the resulting of G-Si cell shows potentially good device parameters including an open-circuit voltage (V_{OC}) of 0.4V and a short-circuit current density (J_{SC}) of 24mA/cm^2, which are both relatively low. The efficiency of this cell can be enhanced by chemical doping or doping by concentrated HNO_3 vapors and coating an antireflection TiO_2 layer. These methods are similar to coating on CNT-Si.

CHAPTER 6

CONCLUSIONS AND PROSPECTS

Graphene is one of the world's most promising materials. It is therefore critical that we can process graphene oxide, graphene hydro-gel, aero-gel and related layers. Utilizing Raman spectroscopy and Fourier Transform Infrared Spectroscopy, the compositional analyses of graphene and graphene related materials has been presented in this study. The micrographs obtained using scanning electron microscopy (SEM) show the structure and morphology of the gel. Electrical measurements have been performed on Graphene/Si.

The graphene gel has a unique 3D network structure. It behaves like a sponge and exhibits super strong absorption towards organic solvents. It has high mechanical strength and is thermally stable (from -200^{o}C to 100^{o}C). Moreover, it is electrically conductive.

It has been reported that graphene gel can be used in drug-delivery, tissue scaffolds, high performance nano-composites and supercapacitors. Graphene is innoxious; therefore, it can be put into human body as carriers of medicine or substitute of organs.

In order to realize the large-scale manufacture of high quality graphene sheets, the approach is to improve synthetic techniques.

Graphene/Silicon should be an ideal material configuration to make solar cells as graphene has shown great potential for applications in photovoltaics due to its high optical transmittance, electrical conductivity and surface area. But the relatively low conversion efficiency has limited its applications in photovoltaics. There is a way to increase the efficiency by replacing planar silicon wafer with silicon nanowire. Compared to planar silicon, the nanowire can provide more surface area for sun light, and can suppress light reflection. The starting point for this method is to change the structure of silicon. Meanwhile, more attention should be paid to Schottky barrier contacts and PN junctions of graphene on silicon.

When graphene comes in contact with silicon, it not only forms PN junction, but also Schottky barrier. This causes a large parasitic resistance to the current flow. It is the main reason for energy consumption and poor device performance. One of the methods to help reduce the resistance is to do chemical doping with graphene. Xiaochang Miao et al doped graphene with bis (trifluoromethanesulfonyl)-amide [((CF3SO2)2NH)] (TFSA) to increase the device power conversion efficiency to 8.6% [36]. Besides, HNO_3 doping can also increase the efficiency to a certain extent. Thus, doping and coatings on graphene/Si is a way to control the PN junction performance of graphene.

APPENDIX A

SEM IMAGES OF GRAPHENE SOL-GEL INTERIOR MICROSTRUCTURES

These are the SEM micrographs with different magnifications of graphene sol-gel.

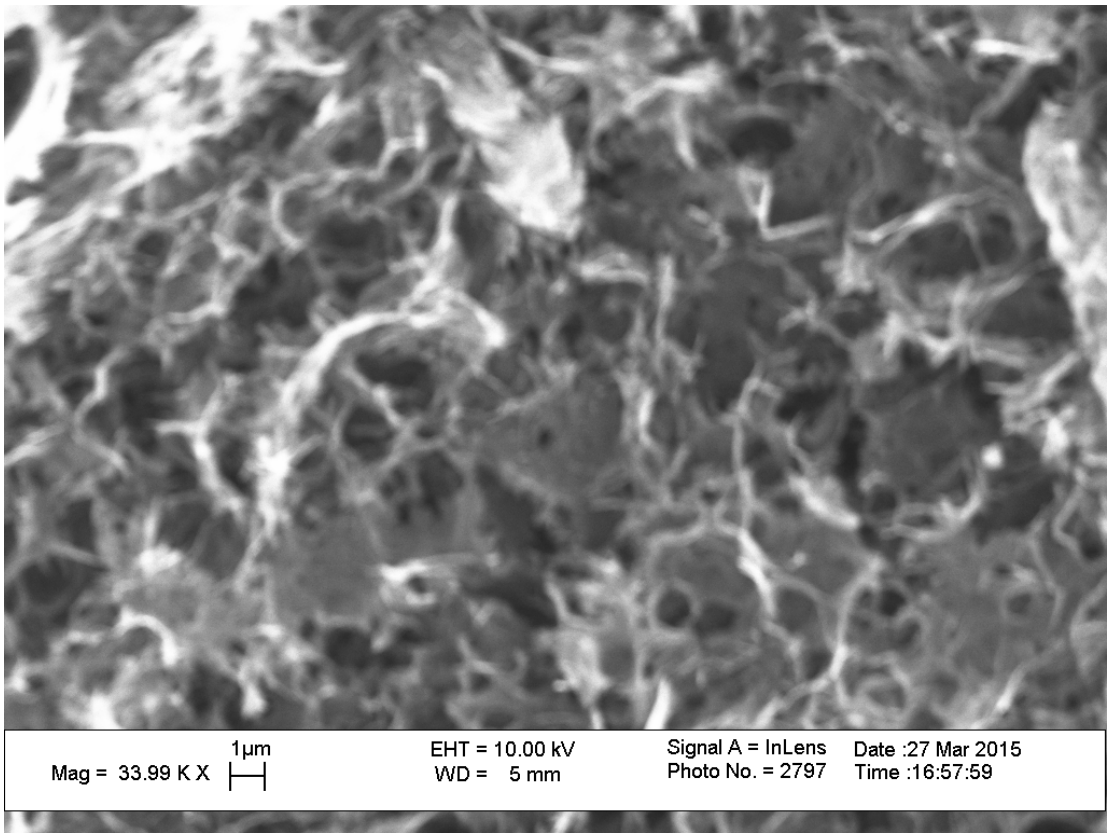

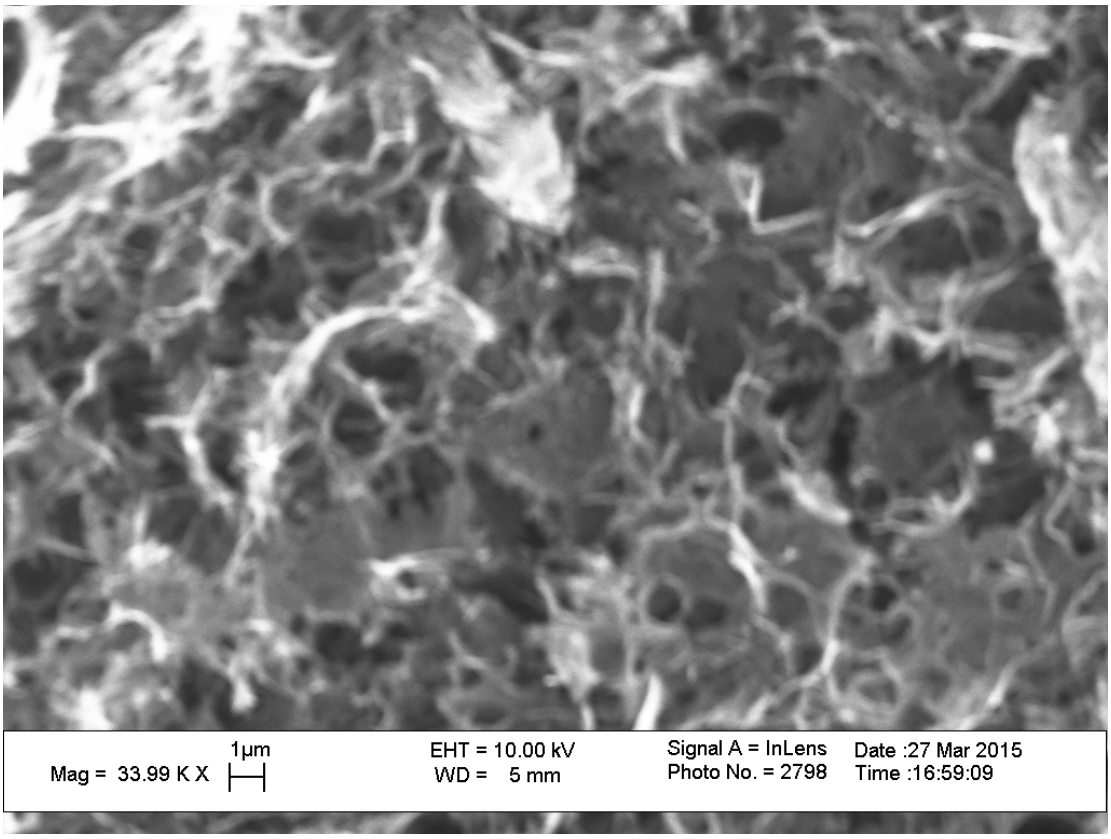
1µm
Mag = 33.99 K X
EHT = 10.00 kV
WD = 5 mm
Signal A = InLens
Photo No. = 2798
Date :27 Mar 2015
Time :16:59:09

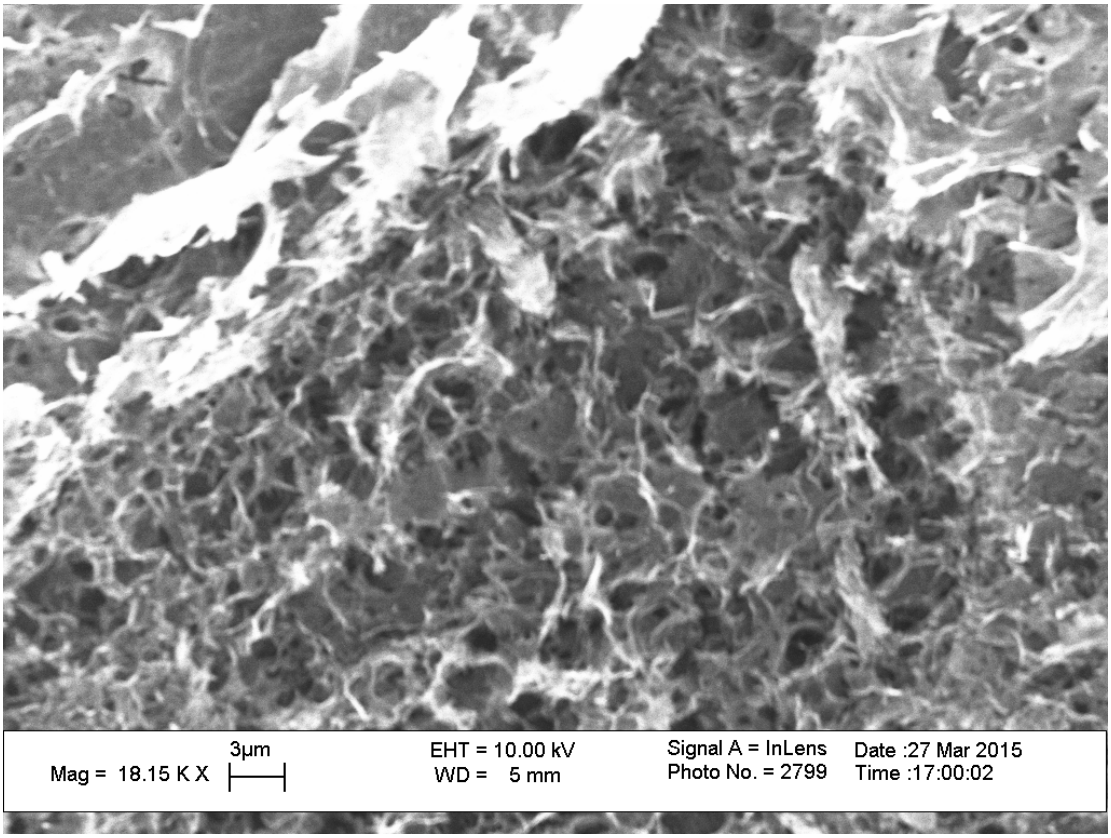
3µm
Mag = 18.15 K X
EHT = 10.00 kV
WD = 5 mm
Signal A = InLens
Photo No. = 2799
Date :27 Mar 2015
Time :17:00:02

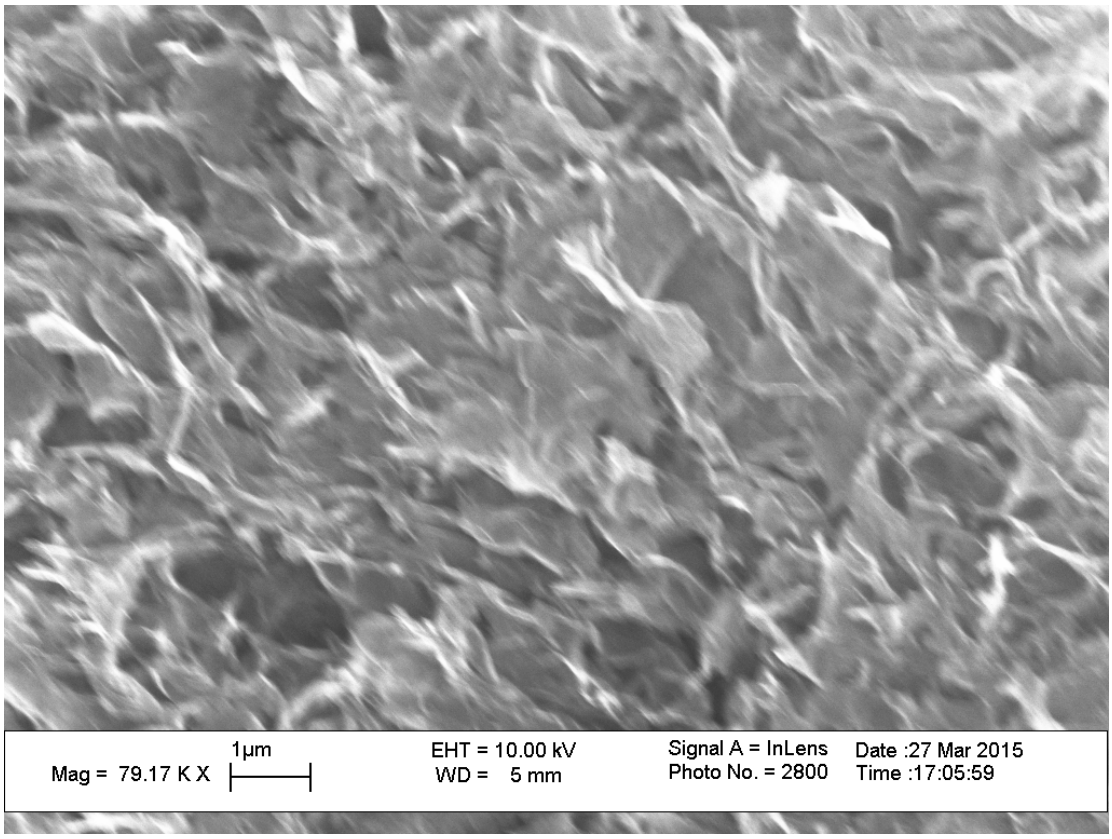
1µm
Mag = 79.17 K X
EHT = 10.00 kV
WD = 5 mm
Signal A = InLens
Photo No. = 2800
Date :27 Mar 2015
Time :17:05:59

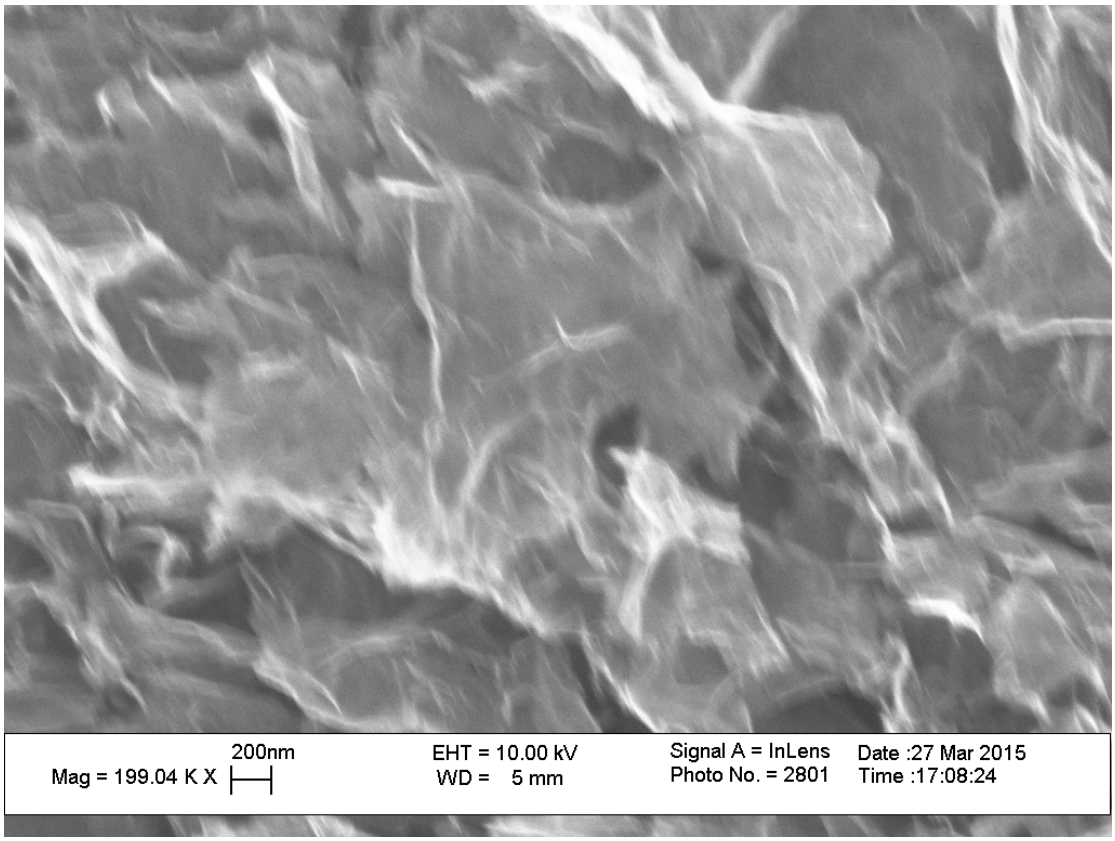
200nm
Mag = 199.04 K X
EHT = 10.00 kV
WD = 5 mm
Signal A = InLens
Photo No. = 2801
Date :27 Mar 2015
Time :17:08:24

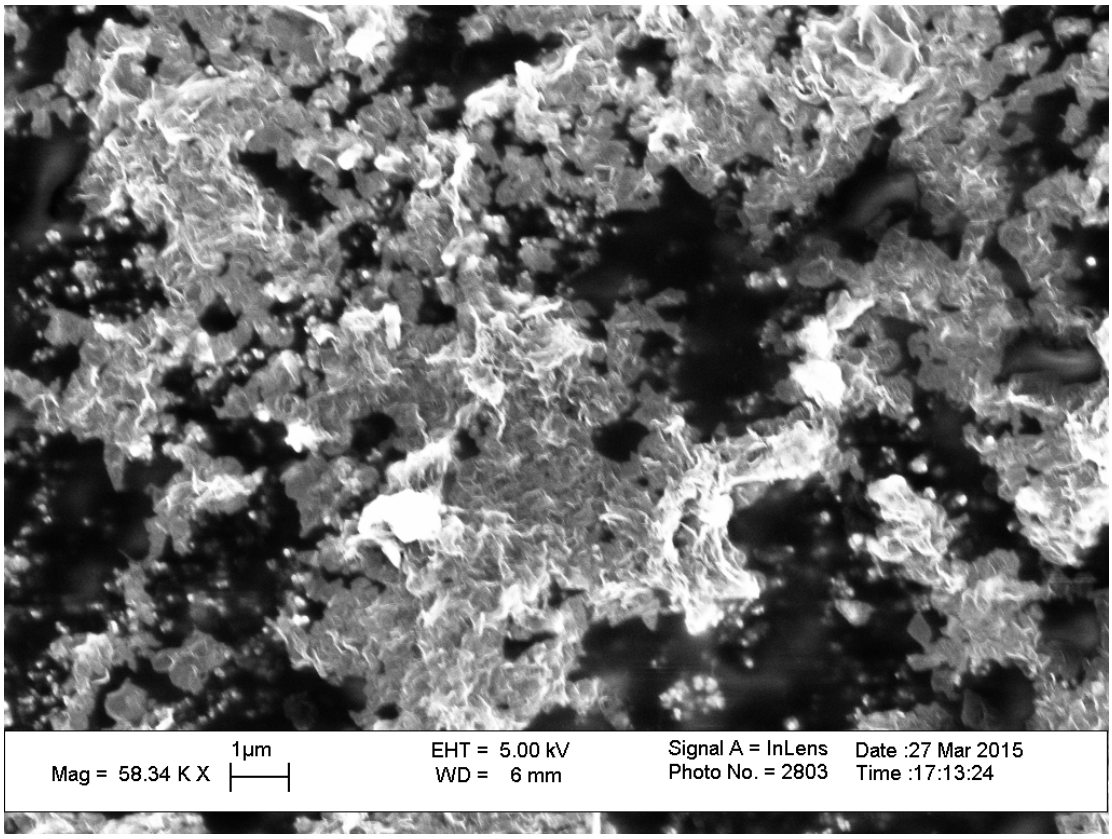
1µm
Mag = 58.34 K X
EHT = 5.00 kV
WD = 6 mm
Signal A = InLens
Photo No. = 2803
Date :27 Mar 2015
Time :17:13:24

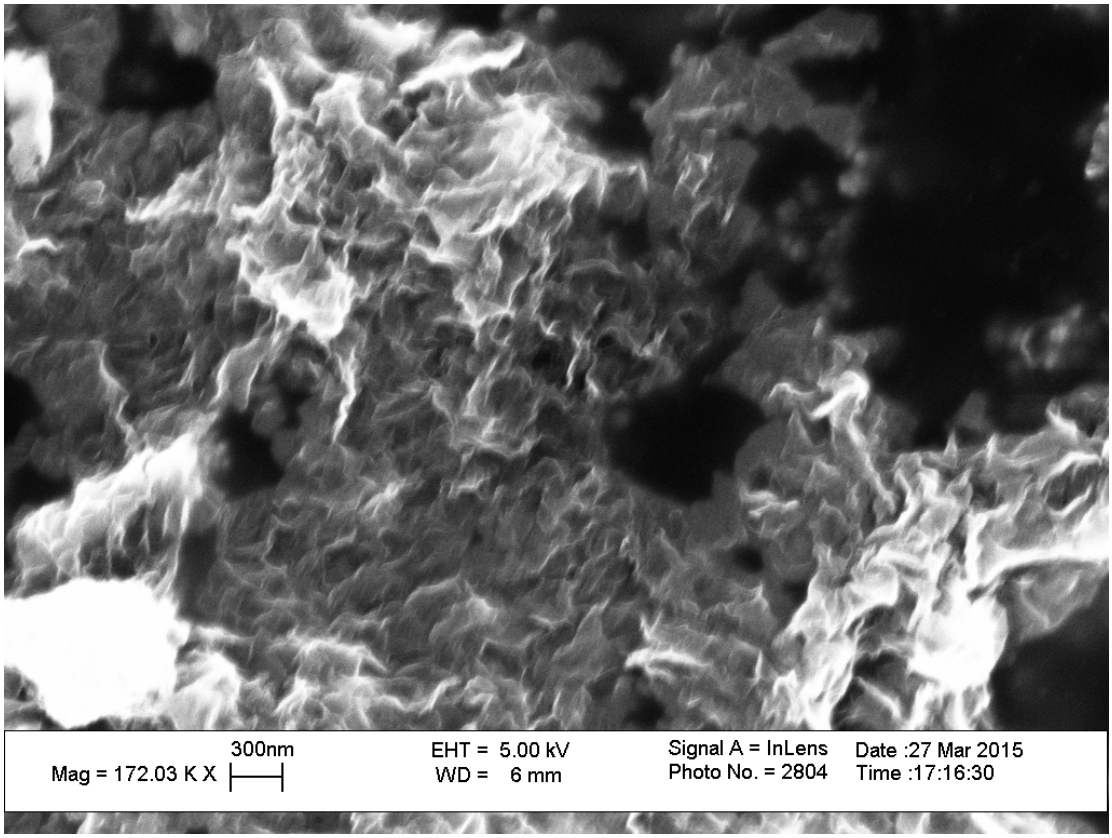
300nm
Mag = 172.03 K X
EHT = 5.00 kV
WD = 6 mm
Signal A = InLens
Photo No. = 2804
Date :27 Mar 2015
Time :17:16:30

APPENDIX B

PRESENTATION SLIDES

These are the presentation slides of my thesis defense.

PROCESSING AND CHARACTERIZATION OF SOL-GEL BASED GRAPHENE AND GRAPHENE ON SILICON

Major: Materials Science & Engineering

Student: Cheng Peng

Advisor: N. M. Ravindra

Abstract

Graphene has become a promising material of many areas including electronic devices, batteries and space crafts. Although it has a bright future, the commercial production of graphene is still not realized.

In this thesis, graphene oxide (GO) and graphene sol-gel are successfully made by proper process in our lab using graphite. Besides, graphene layer is coated on the surface of a silicon wafer. The products are characterized by Raman spectra and FTIR to see its composition. J-V test is carried out to observe the electric property of graphene on silicon. Conclusion and discussion are made based on the test results. At last, the confidence and vision of graphene applications in the future are brought out.

Outline

- Introduction
- Experiment methods
- Experiment process
- Characterization techniques
- Test results
- Conclusion
- Future work

Introduction

What is graphene?

- Graphene is an allotrope of carbon in the form of a two-dimensional, atomic-scale, hexagonal lattice in which one atom forms each vertex. It is the basic structural element of other allotropes, including graphite, charcoal, carbon nanotubes and fullerenes.
- In 1859, Benjamin Collins Brodie[1] was aware of the highly lamellar structure of thermally reduced graphite oxide.

[1] Geim, A. K. (2012). "Graphene Prehistory". Physica Scripta T146: 014003. doi:10.1088/0031-8949/2012/T146/014003.

Introduction

Structure:

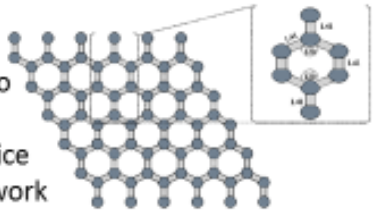

The graphene honeycomb lattice is composed of two equivalent sub-lattices of carbon atoms bonded together with σ bonds. Each carbon atom in the lattice has a π orbital that contributes to a delocalized network of electrons.

By Monte Carlo simulation and transmission electron microscopy (TEM), we know that freely suspended graphene has 'intrinsic' ripples. Apart from 'intrinsic' corrugations, graphene in real 3D space can have other 'defects', including topological defects, vacancies, adatoms, edges/cracks, adsorbed impurities, and so on.

Introduction

Properties

- Electronical : In graphene, the effective mass of electron and electron hole equals zero, which causes the excellent and steady conductibility. Both electrons and charge carriers can transport in graphene freely. Leading to its ultra-high conductivity. (resistivity: Graphene 10^{-6} Ω·cm, Silver 1.59×10^{-6} Ω·cm)
- Mechanical: Graphene has been proved to be the world's toughest material. (200 times higher than steel)
- Optical: The visible light transmittance of Single-layer graphene is up to 97.7%, and it has a linear relationship with the number of layers.
- Thermal: The thermal conductivity of graphene is about 10 times higher than copper. (Graphene:5300W/mK, Copper:401W/mK)

Introduction

Potential applications:

- Flexible screen
- New energy battery
- Ultra-light aircraft materials

Experiment Methods

Preparation of graphene:

- Physical ways: mechanical cleavage method,
  epitaxy growth method,
  Liquid & gas phase dissection method.
- Chemical ways: chemical vapor deposition (CVD),
  graphite oxide reduction method.

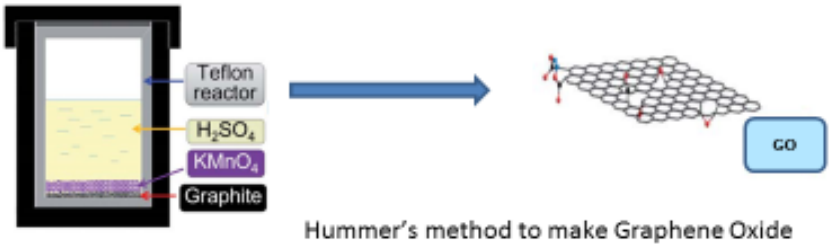

Hummer's method to make Graphene Oxide

Interdisciplinary Program in Materials Science & Engineering

Experiment

Gaphene Oxide was prepared basically using hummer's method, meanwhile, we also changed something to improve it.

1. Concentrated H_2SO_4 (69 mL) was added to a mixture of graphite flakes (3.0 g, 1 wt equiv) and $NaNO_3$ (1.5 g, 0.5 wt equiv), and the mixture was cooled to 0°C using ice water bath.
2. $KMnO_4$ (15-18 g, 5-6 wt equiv) was added slowly with a funnel in portions to keep the reaction temperature below 20°C.
3. The reaction was warmed to 35°C and stirred for 6 hours, at which time water (138 mL) was added slowly with a separatory funnel, producing a large exotherm to 98°C.
4. External heating was introduced by hot water bath to maintain the reaction temperature at 98°C for 15 minutes, then the heat was removed and the reaction was cooled using a water bath until the temperature dropped down below 10°C.
5. Additional water (420 mL) and 30% H_2O_2 (3 mL) were added, producing another exotherm. With the added H_2O_2, the suspension liquid turned golden yellow.
6. After air cooling, hydrochloric acid (HCl) was added in the mixture to remove the rest H_2O_2. Centrifuge was used to wash GO with anhydrous ethanol as solvent for three to five times, until the PH approached 7. Upper clear liquid was removed and left the mud-like graphene oxide.
7. Took out the GO and spread it on a tinfoil in a tray. Put the tray into the vacuum oven at the temperature of 40°C for 24 hours. Then the GO product was prepared.

Experiment

Processing of GO

Experiment

Hydrogel:

GO powders were added in deionized water. Use ultra-sounded and strong mechanical stirring for 2 hours to make it into GO aqueous dispersion (2mg/ml). Put 10ml GO aqueous dispersion in a glass vial. Then, 40mg sodium ascorbate was added. After sonication for 5 minutes to dissolve the sodium ascorbate, a homogeneous yellow-brown dispersion was obtained. Heat this dispersion in a drying oven at 90°C for 1.5 hours to produce the self-assembled graphene hydrogel.

Experiment

Aerogel:

Put the graphene hydrogel in ammonia in room temperature for 24 hours. Then lyophilize it in a freezing dryer. Then graphene aerogel was prepared.

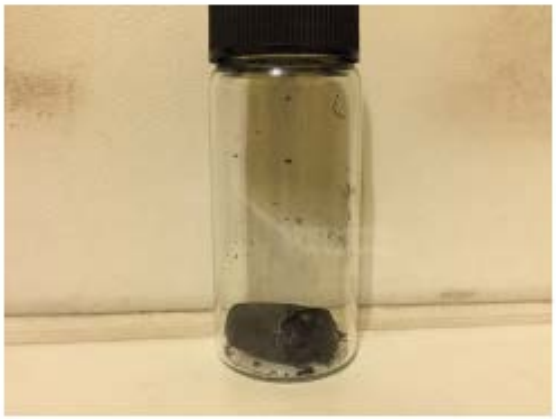

Experiment

Coating on silicon wafer

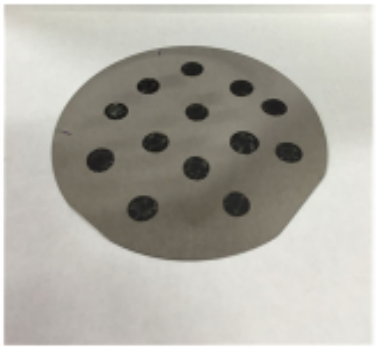

4.0g of GO was dispersed in 1.5L of acetic acid. This dispersion was ultra-sounded using an ultrasonic bath until it became clear. Hydriodic acid (80.0 ml) was then added and the mixture was stored at 40 °C for 40 hours with constant stirring. Then the product was isolated by filtration, washed with saturated sodium bicarbonate (5×100 ml), distilled water (5×100 ml) and acetone (2×100 ml). Use ultrasonic bath again to make a homogeneous liquid dispersion. Drop small droplets on the surface of the silicon wafer where we wanted to.

Characterization techniques

- Raman Spectrum
- Fourier Transform Infrared Spectroscopy (FTIR)
- Scanning Electron Microscopy (SEM)
- Current Density- Voltage (J-V) Test

Results - Raman

The first-order D peak itself is not visible in pristine graphene because of crystal symmetries. While in GO, the charge carrier is excited and inelastically-scattered by a phonon. The prominent D peak at ~1480cm^{-1} and the G peak ~1750cm^{-1} are indicative of significant structural disorder in GO. Weak and broad 2D peaks are another indication of disorder. As the GO product we made had very small crystal size, the amount of disorder can be very high, which leads to very strong D peaks.

Raman Spectrum of GO after the baseline correction.

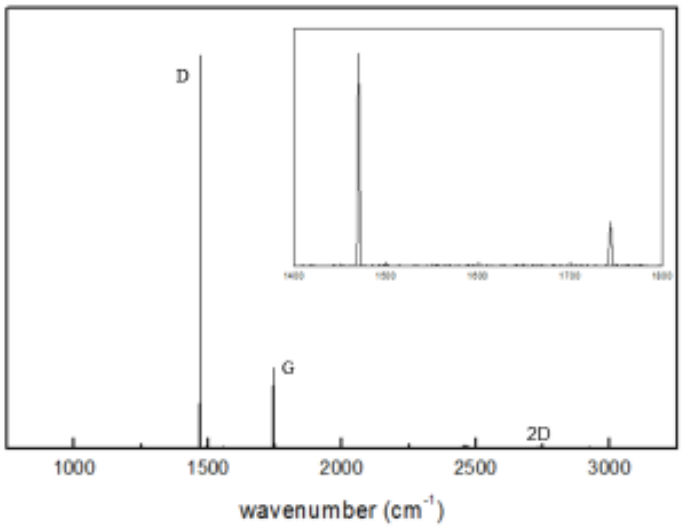

Results - Raman

In Graphene Oxide, The main features in the Raman spectra are the G and D peaks and their overtones. As shown in Figure, the first-order G and D peaks, both arising from the vibrations of sp2 carbon, appear at around 1580 cm-1 and 1350 cm-1, respectively. The G peak corresponds to the optical E2g phonons at the Brillouin zone center resulting from the bond stretching of sp2 carbon pairs in both, rings and chains. G peak would also increase with the larger number of layers. The D peak represents the breathing mode of aromatic rings arising due to the defect in the sample. Therefore, the D peak intensity is often used as a measure for the degree of disorder. The 2D peak is attributed to double resonance transitions resulting in the production of two phonons with opposite momentum.

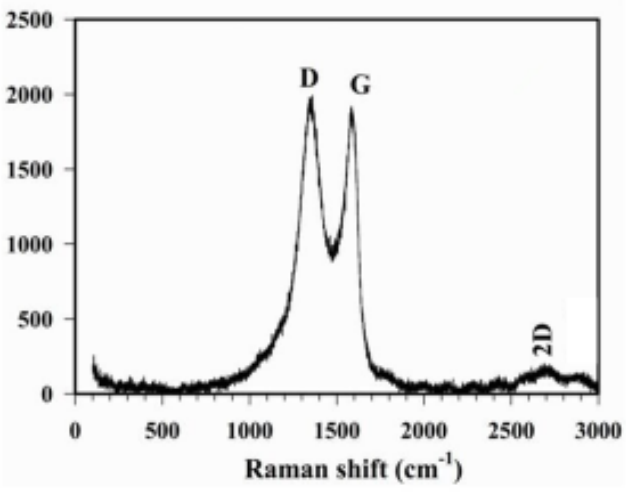

Results - FTIR

Analysis of Fourier Transform Infrared Spectroscopy

The presence of these oxygen-containing groups reveals that the graphene has been successfully oxidized. The polar groups, especially the surface hydroxyl groups, result in the formation of hydrogen bonds between graphite and water molecules; this further explains the hydrophilic nature of graphene oxide.

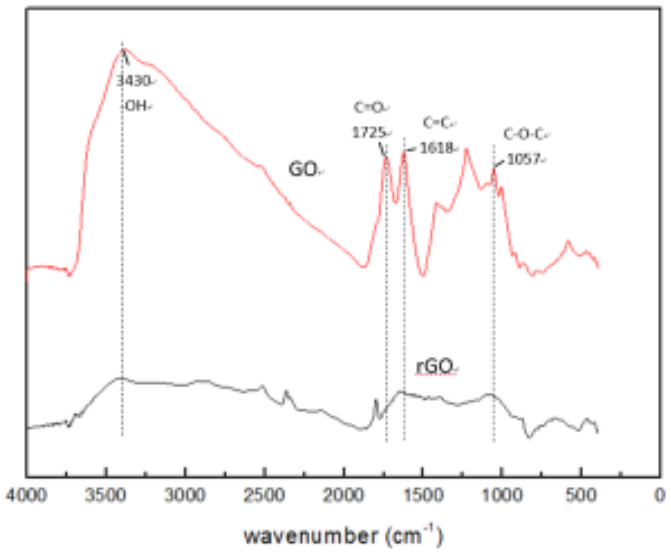

Results - FTIR

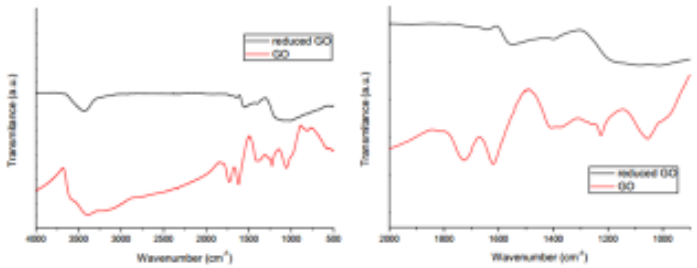

The presence of different type of oxygen functionalities in graphene oxide was confirmed at 3430 cm^{-1} (-OH stretching vibrations), at 1725 cm^{-1} (stretching vibrations from C=O), at 1618 cm^{-1} (skeletal vibrations from unoxidized graphitic domains), at 1225 cm^{-1} (C-OH stretching vibrations), and at 1057 cm^{-1} (C-O stretching vibrations). FTIR peak of reduced graphene presents that -OH stretching vibrations observed at 3430 cm^{-1} was significantly reduced due to deoxygenation. While stretching vibrations from C=O at 1720 cm^{-1} were still observed, which were caused by the remaining carboxyl groups.

Results - SEM

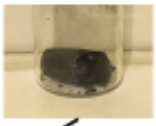

SEM of Sol-Gel based Graphene

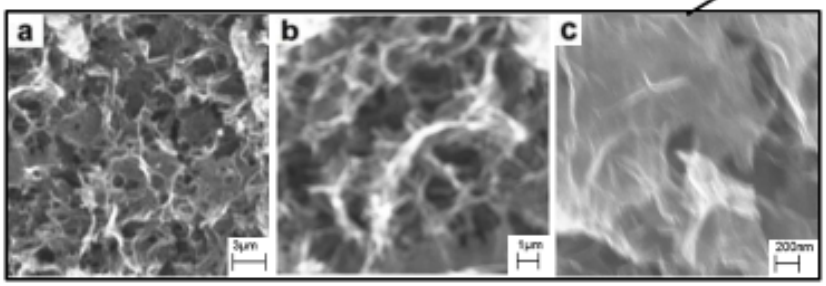

The sol-gel has a well-defined and interconnected 3D porous network as imaged by SEM. The pore sizes are from less than 1micrometer to several micrometers. The walls of the pores are composed of stacked graphene sheets, which contribute to the cross-linked structure of graphene sol-gel. This structure is also the main reason why the sol-gel is so light in weight and flexible.

Results – Graphene/Si

J–V characteristics of Graphene on Silicon

the resulting of G-Si cell shows potential device parameters including an open-circuit voltage (VOC) 0.4V and a short-circuit current density (JSC) of 24mA/cm2, which are both relatively low, though.

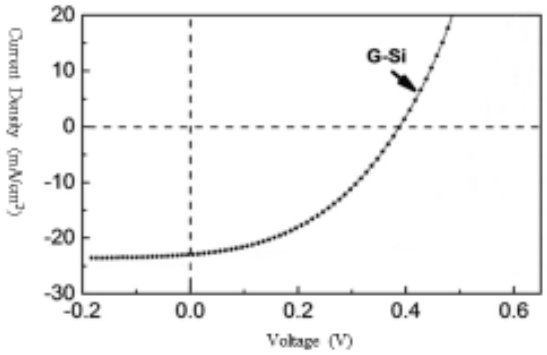

Conclusion

With Raman spectrum and FTIR analysis, products have been proved successfully made. Meanwhile, the photos taken by SEM make me understand more about the structure of the sol-gel, so that the wider use of it can be figured out.

On the other hand, Graphene solar cell has a lot of advantages compared with traditional ones, such as the quicker charge speed, larger changer capacity, lighter in weight and flexible. But right now all the graphene based cells are only exist in labs.

In this thesis, we made the graphene/silicon cell test, as a start in the field of graphene battery.

Future work

Graphene/Silicon should be an ideal structure to make solar cells as graphene has shown great potential for solar cell applications. This is due to its high optical transmittance, electrical conductivity, and surface area. But the relatively low conversion efficiency has limited its application.

When graphene is in contact with silicon, it has not only PN junction, but also the Schottky Barrier, which causes a large parasitic resistance to the current flow. This is the main reason for energy consumption and losses, thus lowering the device performance. One of the methods to help reduce the resistance/loss is to do chemical doping with graphene.

Structure modification by doping and coating on Graphene/Si is perhaps a way to control the PN junction performance of Graphene. The goal is to achieve enhanced conversion efficiency of Graphene/Si for application in photovoltaics.

REFERENCES

[1] Geim, A. K., Novoselov, K. S., The rise of graphene, *Nature Materials*, **6**,183 -191, (2007).

[2] Meyer, J. C., The structure of suspended graphene sheets, *Nature*, **446**, 60-63, (2007).

[3] Reina, A., Jia, X. T., Ho, J., et al. Large area, few-layer graphene films on ar bitrary substrates by chemical vapor deposition, *Nano Lett*, **9**, 30-35, (2009).

[4] Kim, K. S., et al., Large-scale pattern growth of graphene films for stretchable transparent electrodes, *Nature*, **457**, 706-710, (2009).

[5] Grüneis, A., Vyalikh, D. V., Tunable hybridization between electronic states of graphene and a metal surface, *Physical Review*. B **77**, 193401, (2008).

[6] Fasolino, A., Los, J. H., Katsnelson, M. I., M.I. Intrinsic ripples in graphene, *Nature materials*, **6**, 858, (2007).

[7] Meyer, J. C., Geim, A. K., Katsnelson, M. I., Novoselov, K. S., Booth, T. J., Roth, S., The structure of suspended graphene sheets, *Nature*, **446**, 60-63, (20 07).

[8] Avouris, P., Chen, Z., Perebeinos, V., Carbon-based electronics, *Nature Nanote chnology*, 2, **10**, 605, (2007).

[9] Wallace, P. R., the Band Theory of Graphite, *Physical Review*, **71**, 622, (194 7).

[10] Semenoff, G.W., Condensed-Matter Simulation of a Three-Dimensional Ano maly, *Physical Review Letters*, **53**, 5449, (1984).

[11] Lamas, C. A., Cabra, D. C., Grandi, N., Generalized Pomeranchuk instabiliti es in graphene, *Physical Review* B, 80, **7**, 75108, (2009).

[12] Chen, J. H., Jang, C., Xiao, S., Ishigami, M., Fuhrer, M.S., Intrinsic and Ext rinsic Performance Limits of Graphene Devices on SiO_2, *Nature Nanotechnolo gy*, **3**, 206–209, (2008).

[13] Kuzmenko, A. B., Heumen, E. V., Carbone, F., Marel, D. V. D., Universal in frared conductance of graphite. *Physical Review Letters* 100, **11**, 117401, (200 8).

[14] Kurum, U., Liu, B., Zhang, K. L., Liu, Y., Zhang, H., Electrochemically tun able ultrafast optical response of graphene oxide, *Applied Physics Letters* 98, **2**, 141103, (2011).

[15] Coxworth, B., Imperfect graphene may be perfect for use in better fuel cells, *Science*, (2015).

[16] Novoselov, K. S., Geim, A. K., Morozov, S. V., Jiang, D., Zhang, Y., Dubon os, S. V., Grigorieva, I. V., Firsov, A. A., Electric Field Effect in Atomically Thin Carbon Films, *Science*, **306**, 666−669, (2004).

[17] Sutter, P. W., Flege, J. I., Sutter, E. A., Epitaxial graphene on ruthenium, *Na ture Materials*, **5**, 406−411, (2008).

[18] Hernandez, Y., Nicolosi, V., Lotya, M., Blighe, F. M., Sun, Z., De, S., McG overn, I. T., Holland, B., Byrne, M., Gun'Ko, Y. K., Boland, J. J., Niraj, P., Duesberg, G., Krishnamurthy, S., Goodhue, R., Hutchison, J., Scardaci, V., F errari, A. C., Coleman, J. N., High-yield production of graphene by liquid-ph ase exfoliation of graphite, *Nature Nanotechnology*, **7**, 563−568, (2008).

[19] Srivastava, S. K., Shukla, A. K., Vankar, V. D., Kumar, V., Growth, structure and field emission characteristics of petal like carbon nano-structured thin fi lms, *Thin Solid Films*, **492**, 124−130, (2005).

[20] Staudenmaier, L., Verfahren zur Darstellung der Graphitsäure, *Ber. Dt. Sch. Ch em. Ges.*, **31**, 1481−1487, (1898).

[21] Brodie, B. C., Sur le poids atomique du graphite, *Ann. Chim. Phys.*, **59**, 466−4 72, (1860).

[22] Hummers, W. S., Offeman, R. E., Preparation of Graphitic Oxide, *J. Am. Che m. Soc.*, **80**, 1339−1339, (1958).

[23] Marcano, D. C., Kosynkin, D. V., Berlin, J. M., Slesarev, A., Alemany, L. B., Lu, W., Tour, J. M., Improved Synthesis of Graphene Oxide, *AcsNano*, 4, **8**, 4806-4814, (2010).

[24] Mann, S., Self-Assembly and Transformation of Hybrid Nano-Objects and N

anostructures under Equilibrium and Non-Equilibrium Conditions. *Nat. Mater*, **8**, 781–792, (2009).

[25] Gao, Y., Tang, Z., Design and Application of Inorganic Nanoparticle Superstr uctures: Current Status and Future Challenges. *Small*, **7**, 2133–2146, (2011).

[26] Sheng, K. X., Xu, Y. X., Li, C., Shi, G. Q., High-performance self-assemble d graphene hydrogels prepared by chemical reduction of graphene oxide, *Ne w Carbon Materials*, **2**, 9-15, (2011).

[27] Sun, H. Y., Xu, Z., Gao, C., Multifunctional, Ultra-Flyweight, Synergistically Assembled Carbon Aerogels, *Advanced Materials*, May 14, 2554–2560, (201 3).

[28] Moon, I. K., Lee, J., Ruoff, R. S., Lee, H., Reduced graphene oxide by che mical graphitization, *Nature Communications*, 1:73, doI: 10.1038/ncomms106 7, (2010).

[29] Pop, E., Mann, D., Wang, Q., Goodson, K., Dai, H., Thermal conductance of an individual single-wall carbon nanotube above room temperature. *Nano Le tters*. 6, **1**, 96–100, (2005).

[30] Gardiner, D. J., Practical Raman spectroscopy. Springer-Verlag, ISBN 978-0-38 7-50254-0, (1989).

[31] Griffiths, P., de Hasseth, J. A., Fourier Transform Infrared Spectrometry (2nd edition). Wiley-Blackwell. ISBN 0-471-19404-2, (2007).

[32] Saito, R., Hofmann, M., Dresselhaus, G., Jorio, A., Dresselhaus, M. S., Ram an spectroscopy of graphene and carbon nanotubes. *Adv. Phys*. **30**, 413-550, 2011.

[33] Shahriary, L., Athawale, A. A., Graphene Oxide Synthesized by using Modif ied Hummers Approach, International Journal of Renewable Energy and Envi ronmental Engineering, ISSN 2348-0157, 02, **01**, (2014).

[34] Nanoinnova Technologies SL http://www.nanoinnova.com/Uploads/Features/76 65255.pdf (accessed March 10, 2015)

[35] Shi, E. Z. et al, Colloidal Antireflection Coating Improves Graphene − Silico n Solar Cells, *Nano Letters*, **13**, 1776-1781, (2013).

[36] Miao, X. Ch. et al, High Efficiency Graphene Solar Cells by Chemical Dopi ng, *Nano Letters*, **12**, 2745-2750, (2012).